JOURNAL OF GEOPHYSICAL RESEARCH, VOL. 113, C07003, doi:10.1029/2007JC004558, 2008

Arctic sea ice variability and trends, 1979–2006

Claire L. Parkinson[1] and Donald J. Cavalieri[1]

Received 18 September 2007; revised 25 January 2008; accepted 5 March 2008; published 1 July 2008.

[1] Analysis of Arctic sea ice extents derived from satellite passive-microwave data for the 28 years 1979–2006 yields an overall negative trend of −45,100 ± 4,600 km^2/a (−3.7 ± 0.4%/decade) in the yearly averages, with negative ice extent trends also occurring for each of the four seasons and each of the 12 months. For the yearly averages, the largest decreases occur in the Kara and Barents seas and the Arctic Ocean, with linear least squares slopes of −10,600 ± 2,800 km^2/a (−7.4 ± 2.0%/decade) and −10,100 ± 2,200 km^2/a (−1.5 ± 0.3%/decade), respectively, followed by Baffin Bay/Labrador Sea, with a slope of −8000 ± 2000 km^2/a (−9.0 ± 2.3%/decade), the Greenland Sea, with a slope of −7000 ± 1400 km^2/a (−9.3 ± 1.9%/decade), and Hudson Bay, with a slope of −4500 ± 900 km^2/a (−5.3 ± 1.1%/decade). These are all statistically significant decreases at a 99% confidence level. The seas of Okhotsk and Japan also have a statistically significant ice decrease, although at a 95% confidence level, and the three remaining regions, the Bering Sea, Canadian Archipelago, and Gulf of St. Lawrence, have negative slopes that are not statistically significant. The 28-year trends in ice areas for the Northern Hemisphere total are also statistically significant and negative in each season, each month, and for the yearly averages.

Citation: Parkinson, C. L., and D. J. Cavalieri (2008), Arctic sea ice variability and trends, 1979–2006, *J. Geophys. Res.*, *113*, C07003, doi:10.1029/2007JC004558.

1. Introduction

[2] Sea ice is a major component of the Arctic environment that covers approximately 15 × 10^6 km^2 of the north polar and subpolar oceans in midwinter and typically 5–7 × 10^6 km^2 even at its summer minimum. The ice constantly impacts its surroundings by limiting exchanges between the ocean and atmosphere and reflecting most of the solar radiation incident on it. Furthermore, as sea ice forms and ages, salt is rejected to the ocean below, so that sea ice tends to have lower salinity than seawater. Consequently, as the ice forms and melts, the salinity content of the underlying ocean increases and decreases, respectively, impacting overturning and ocean circulation. Furthermore, as the ice moves, it transports its cold, low-salinity mass, affecting surface temperature and salt gradients [*Aagaard and Carmack*, 1989; *Barry et al.*, 1993; *Parkinson*, 1996]. Changes in the sea ice cover hence have potential broad-range climate consequences, as quantified, for instance, by a numerical model in which 37% of the global warming simulated for a doubled CO_2 scenario was attributable explicitly to having a changing sea ice cover included in the calculations [*Rind et al.*, 1995]. Changes in the ice also impact a wide range of Arctic wildlife, including polar bears, who depend on the ice as the platform from which they hunt for their largely marine-based diet [*Derocher et al.*, 2004; *Stirling and Parkinson*, 2006], and Arctic foxes, who follow the polar bears to scavenge the remains of polar bear kills and depend on the ice for traveling between Arctic islands [*Geffen et al.*, 2007].

[3] Several studies done in the past two decades have revealed a trend toward reduced Arctic sea ice coverage since the late 1970s, using a multichannel satellite passive-microwave data record that began with the deployment of the Scanning Multichannel Microwave Radiometer (SMMR) following its launch on NASA's Nimbus 7 satellite in October 1978. A few of these studies are based solely on the SMMR data, extending through mid-1987 [e.g., *Parkinson and Cavalieri*, 1989; *Gloersen and Campbell*, 1991], although most are based also on data from the Defense Meteorological Satellite Program (DMSP) Special Sensor Microwave Imagers (SSMIs), first launched in June 1987 and continuing to the present [e.g., *Johannessen et al.*, 1995; *Maslanik et al.*, 1996; *Bjørgo et al.*, 1997; *Cavalieri et al.*, 1997; *Parkinson et al.*, 1999; *Stroeve et al.*, 2005; *Comiso*, 2006; *Meier et al.*, 2007]. Of the latter studies, *Parkinson et al.* [1999] present extensive analysis of the 18.2-year record of Northern Hemisphere sea ice extents derived from the SMMR and SSMI data for the period from November 1978 through December 1996. The current paper updates the Northern Hemisphere results of *Parkinson et al.* [1999] from an 18.2-year record to a 28.2-year record and places the results in a broader climate context. A companion paper, by *Cavalieri and Parkinson* [2008] provides the corresponding results for the Southern Hemisphere, updating to 28.2 years

[1]NASA Goddard Space Flight Center, Greenbelt, Maryland, USA.

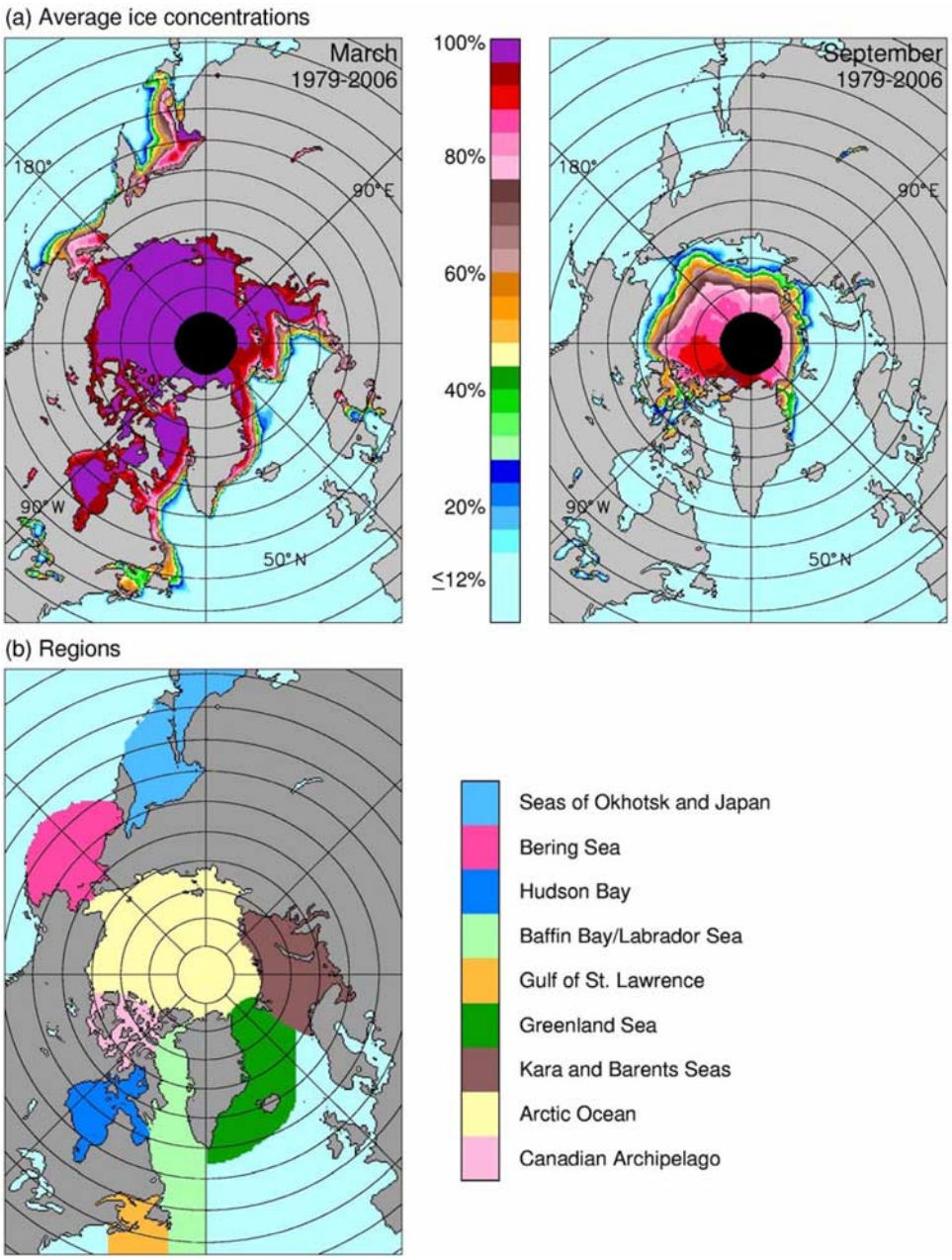

Figure 1. (a) Maps of Northern Hemisphere March and September sea ice concentrations, averaged over the years 1979–2006, as derived from satellite passive-microwave observations. (b) Location map of the regions used in the analysis.

the 20.2-year Southern Hemisphere results reported by *Zwally et al.* [2002].

2. Data

[4] The data used in this study are derived from NASA's Nimbus 7 SMMR for the period November 1978 through July 1987 and the DMSP F8, F11, and F13 SSMIs for the period August 1987 through December 2006. SMMR was operational on an every-other-day basis for most of the period from 26 October 1978 through 20 August 1987; and the SSMIs were operational on a daily basis for most of the period from 9 July 1987 through the end of December 2006 and beyond. The reader is referred to *Cavalieri et al.* [1999] for details on the creation of the 1978–1996 data set of sea ice concentrations (percent areal coverages of ice), which have been updated using the same methodology. The Northern Hemisphere ice concentrations are mapped to a common rectangular grid overlaid on a north polar stereographic projection with a grid cell size of 25 km × 25 km [*NSIDC*, 1992]. This sea ice concentration data set, available from the National Snow and Ice Data Center (NSIDC), was the source data for the calculation of sea ice extents (cumulative areas of all grid cells having at least 15% sea ice concentration) and sea ice areas (sums of the pixel areas times the ice concentrations for all pixels with ice concentrations of at least 15%). The 15% threshold is widely used for both ice extent and ice area

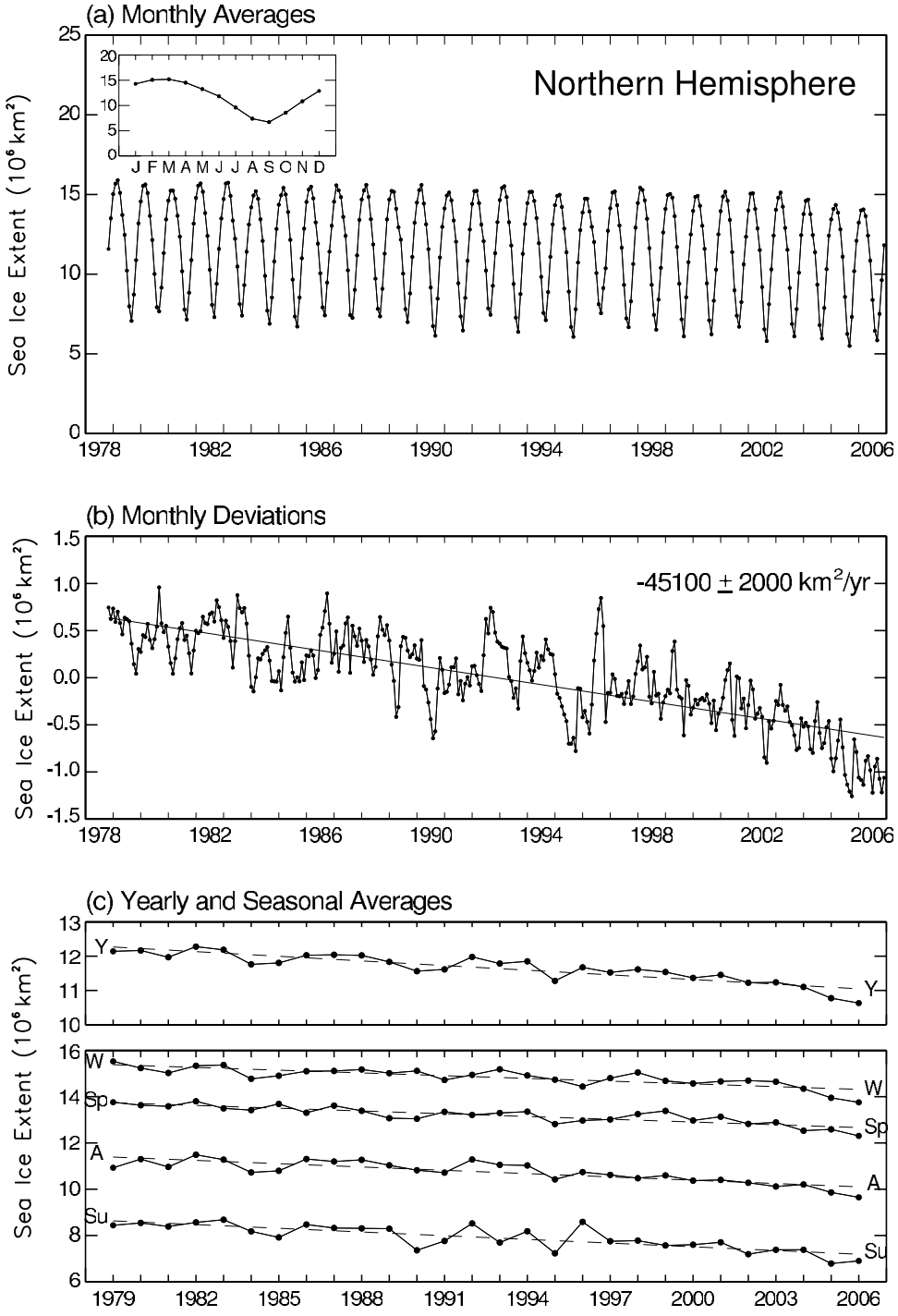

Figure 2. (a) Monthly averaged satellite-derived Northern Hemisphere sea ice extents for November 1978 through December 2006, with an inset presenting the average annual cycle. The average cycle reaches a minimum of 6.7 $\times$ 10^6 km^2 in September and a maximum of 15.2 $\times$ 10^6 km^2 in March. (b) Monthly deviations for the sea ice extents of Figure 2a, calculated by taking the monthly value for the individual month and subtracting the average value for that month over the 28.2-year period, plus the line of linear least squares fit through the monthly deviations, along with its slope and estimated standard deviation. (c) Yearly and seasonally averaged sea ice extents for the years 1979–2006. The winter (W), spring (Sp), summer (Su), and autumn (A) values cover the periods January–March, April–June, July–September, and October–December, respectively.

Table 1. Slopes of the Lines of Linear Least Squares Fit Through Yearly and Seasonal Arctic Sea Ice Extents, 1979–2006[a]

Region	Yearly			Winter			Spring			Summer			Autumn		
	10^3 km^2/a	S	%/decade	10^3 km^2/a	S	%/decade	10^3 km^2/a	S	%/decade	10^3 km^2/a	S	%/decade	10^3 km^2/a	S	%/decade
Northern Hemisphere	−45.1 ± 4.6	99	−3.7 ± 0.4	−39.5 ± 5.6	99	−2.6 ± 0.4	−39.7 ± 4.6	99	−2.9 ± 0.3	−53.4 ± 7.9	99	−6.2 ± 0.9	−47.7 ± 6.1	99	−4.2 ± 0.5
Seas of Okhotsk and Japan	−3.8 ± 1.5	95	−8.5 ± 3.3	−8.8 ± 3.8	95	−7.7 ± 3.3	−5.3 ± 2.3	95	−11.2 ± 4.8	0.0 ± 0.0		0.0 ± 0.0	−1.0 ± 0.9		−6.0 ± 5.5
Bering Sea	−0.5 ± 1.0		−1.6 ± 3.1	0.5 ± 2.2		0.7 ± 3.3	−1.3 ± 1.9		−3.5 ± 5.2	−0.1 ± 0.0	99	−22.6 ± 2.7	−1.0 ± 1.1		−5.8 ± 6.0
Hudson Bay	−4.5 ± 0.9	99	−5.3 ± 1.1	−0.0 ± 0.0		−0.0 ± 0.0	−3.4 ± 0.8	99	−2.8 ± 0.7	−5.8 ± 1.5	99	−19.5 ± 5.0	−8.5 ± 1.9	99	−12.9 ± 2.9
Baffin Bay/Labrador Sea	−8.0 ± 2.0	99	−9.0 ± 2.3	−10.0 ± 3.9	95	−6.9 ± 2.7	−8.9 ± 2.6	99	−7.6 ± 2.2	−4.6 ± 1.4	99	−16.0 ± 4.8	−8.5 ± 1.8	99	−12.5 ± 2.7
Gulf of St. Lawrence	−0.3 ± 0.3		−3.7 ± 4.4	−1.5 ± 1.0		−7.2 ± 4.6	−0.0 ± 0.4		−0.3 ± 5.4	0.0 ± 0.0		0.0 ± 0.0	0.4 ± 0.2	95	10.7 ± 4.5
Greenland Sea	−7.0 ± 1.4	99	−9.3 ± 1.9	−9.9 ± 2.4	99	−10.0 ± 2.5	−6.4 ± 1.5	99	−7.4 ± 1.8	−5.4 ± 2.0	95	−11.4 ± 4.3	−6.4 ± 1.8	99	−9.2 ± 2.6
Kara and Barents Seas	−10.6 ± 2.8	99	−7.4 ± 2.0	−9.5 ± 2.9	99	−5.1 ± 1.5	−12.4 ± 4.0	99	−6.9 ± 2.2	−11.2 ± 3.6	99	−15.5 ± 5.0	−9.1 ± 3.0	99	−7.0 ± 2.3
Arctic Ocean	−10.1 ± 2.2	99	−1.5 ± 0.3	−0.2 ± 0.1		−0.0 ± 0.0	−1.7 ± 0.8	95	−0.2 ± 0.1	−25.6 ± 6.0	99	−4.1 ± 1.0	−12.4 ± 2.7	99	−1.8 ± 0.4
Canadian Archipelago	−0.5 ± 0.4		−0.7 ± 0.6	−0.0 ± 0.0		−0.0 ± 0.0	−0.3 ± 0.2		−0.4 ± 0.2	−0.8 ± 1.2		−1.4 ± 2.2	−0.9 ± 0.4		−1.2 ± 0.6

[a]In units of 10^3 km^2/a and %/decade, with estimated standard deviations and an indication (column S) of which values are statistically significant at the 99% and 95% confidence levels. (The rates of change are calculated from the starting point to the ending point of the least squares fit line, with the starting point being the reference.)

calculations and in particular was used in the *Parkinson et al.* [1999] study. The need for some non-0% threshold is multifaceted: (1) physically, inclusion of random ice floes well equatorward of the main ice pack would not provide a realistic indication of the ice coverage; (2) atmospheric interference with the microwave signal produces many regions well outside of the ice pack where the ice concentration calculations erroneously suggest a small amount of ice, predominantly under 15%. Choosing a 15% threshold for ice coverage removes by far the majority of the atmospheric interference while still retaining in the calculations and results the overwhelming majority of the ice cover. Hence we follow convention and retain the 15% threshold.

[5] In the calculation of ice extents, we adjust for the consistent lack of SMMR data poleward of 84.6°N and SSMI data poleward of 87.6°N by assuming that both these regions are ice covered throughout to a concentration of at least 15%. This is a reasonable assumption in view of the much higher ice concentrations generally surrounding these regions, illustrated, for instance, in maps of the average ice concentrations for the months of maximum and minimum sea ice coverage, March and September, respectively (Figure 1a). In the calculation of ice areas, we assume 100% ice coverage poleward of 84.6°N, which introduces an error in view of the presence of an unknown but presumably small amount of leads in this vicinity. Because of our uniform application of the assumption of 100% ice coverage poleward of 84.6°N, our ice area trends are not affected by any changes in this region and are therefore technically the trends for the ice equatorward of 84.6°N.

[6] The ice extents and ice areas were calculated on a daily basis (or every other day in the case of the SMMR data) and then combined to monthly, seasonal, and yearly averages. Monthly deviations were calculated by taking the individual monthly averages and subtracting the 28-year average (or, for November and December, the 29-year average) for that month. Lines of linear least squares fit were determined for the monthly deviations and the seasonal and yearly averages, and the estimated standard deviations (σ) of their slopes were calculated following *Taylor* [1997]. To give a rough indication of the significance of the trends, we use a two-tailed t-test with 26 degrees of freedom (2 less than the number of years) to indicate which slopes are considered statistically significant as nonzero with a 95% confidence level and which are considered significant with a 99% confidence level. These indications are based exclusively on the ratio of the trend to the standard deviation, with ratios above 2.06 being deemed significant at a 95% confidence level and ratios above 2.78 being deemed significant at a 99% confidence level. They give a valuable, although imperfect [e.g., *Santer et al.*, 2000], indication of which trends emerge most clearly above the noise level.

[7] As in the work of *Parkinson et al.* [1999], results are presented for nine regions and their total. The nine regions are the seas of Okhotsk and Japan, the Bering Sea, Hudson Bay, Baffin Bay/Labrador Sea, the Gulf of St. Lawrence, the Greenland Sea, the Kara and Barents seas, the Arctic Ocean, and the Canadian Archipelago (Figure 1b). Their total constitutes the ''Northern Hemisphere'' value, although

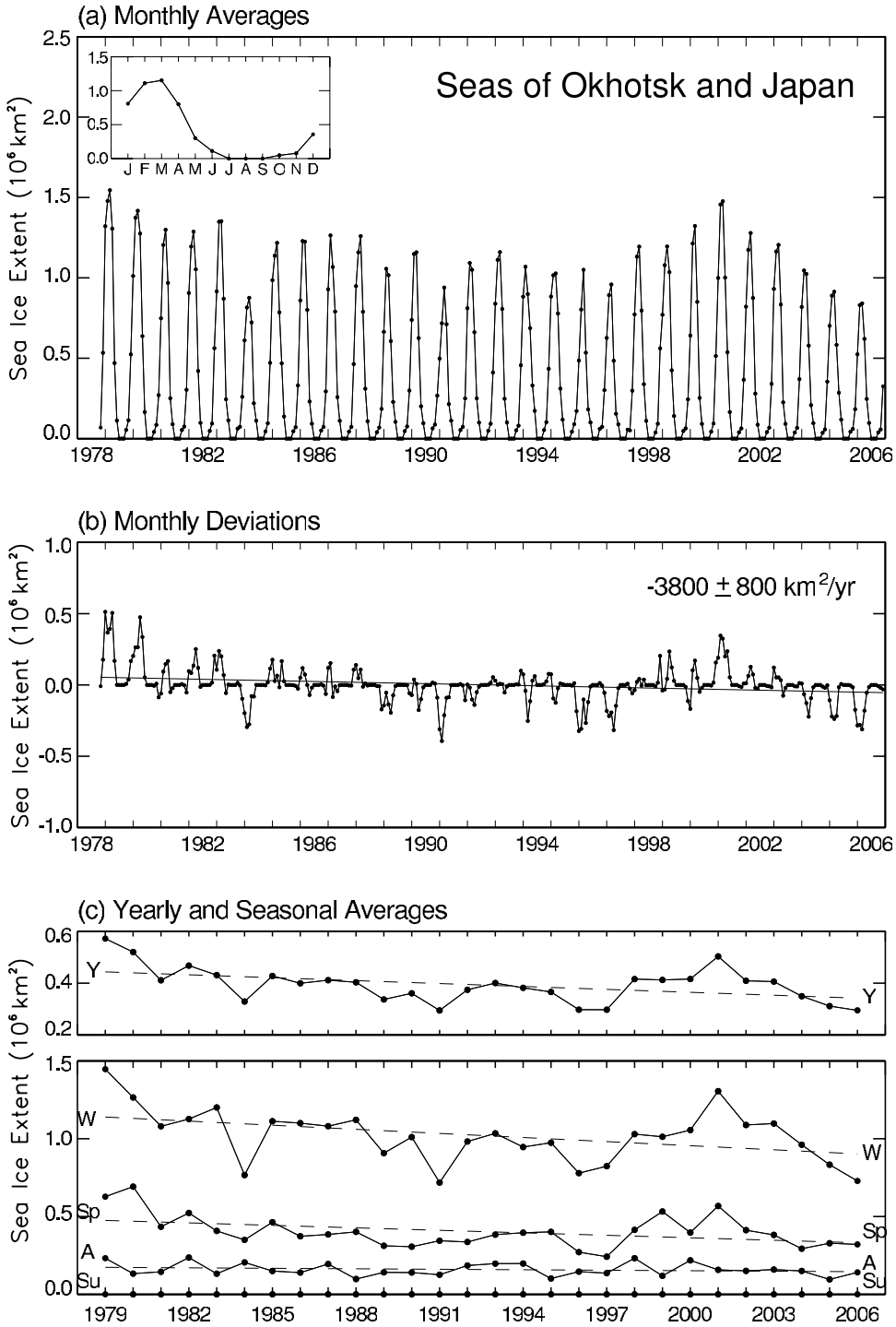

Figure 3. Same as Figure 2, except for the regional values for the seas of Okhotsk and Japan.

some small areas of sea ice coverage lie outside of these nine regions.

3. Results

3.1. Sea Ice Extents

3.1.1. Northern Hemisphere Total

[8] Figure 2 presents plots of monthly average ice extents and monthly deviations from November 1978 through December 2006 and yearly and seasonal averages for 1979 through 2006 for the Northern Hemisphere total. The downward trend of $-34{,}300 \pm 3{,}700$ km^2/a reported for the monthly deviations for November 1978 to December 1996 by *Parkinson et al.* [1999] has been replaced by the much steeper downward trend of $-45{,}100 \pm 2{,}000$ km^2/a for the period through December 2006 (Figure 2b), and indeed none of the deviations in the past 10 years are as high as 0.5×10^6 km^2 and most of the deviations in the last 2 years of the record fall below the lowest of any of the deviations in the initial 18.2-year record (Figure 2b).

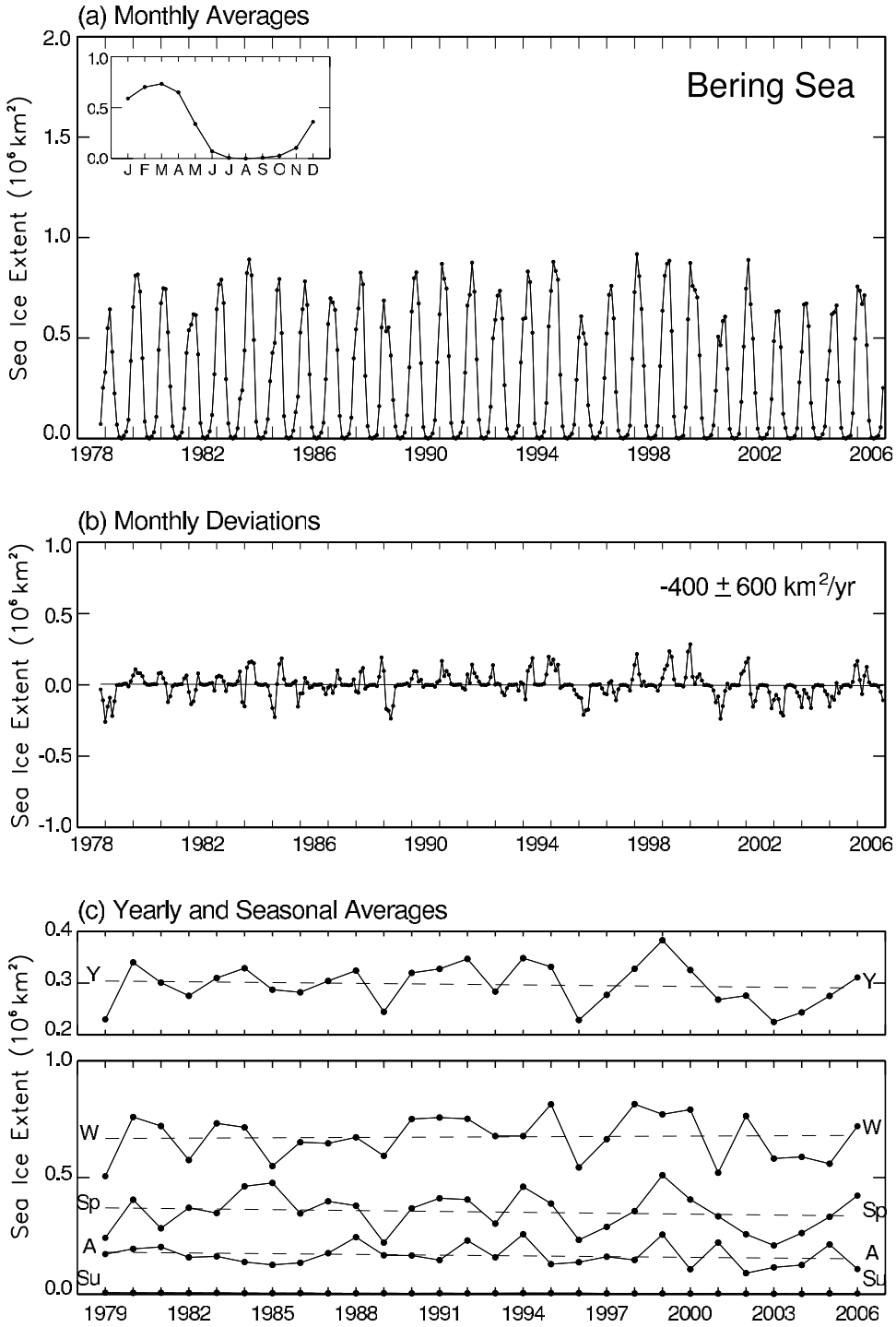

Figure 4. Same as Figure 2, except for the regional values for the Bering Sea.

[9] The slopes of the lines of linear least squares fit through the yearly and seasonal ice extent values plotted in Figure 2c, for the Northern Hemisphere total, are presented in Table 1, along with the corresponding slopes for each of the nine regions. The Northern Hemisphere slope for the yearly averages, $-45{,}100 \pm 4{,}600$ km^2/a, is identical (to three significant figures) to the slope for the monthly deviations (Figure 2b), although has a higher standard deviation, reflective of the smaller number of data points (28 years versus 28 × 12 + 2 months). Seasonally, the highest-magnitude slope is for the summer values, at $-53{,}400 \pm 7{,}900$ km^2/a, with the next strongest trend being for autumn; but even the weakest seasonal trend, at $-39{,}500 \pm 5{,}600$ km^2/a for winter, is considered statistically significant at a 99% confidence level, as are the trends for each of the other seasons (Table 1). With the 18-year record through 1996, the strongest seasonal slope had been at $-42{,}800 \pm 7{,}500$ km^2/a for the spring values, and only the spring and winter seasons had statistical significance at 99% [*Parkinson et al.*, 1999]. Interestingly, with the additional 10 years of data, the 28-year spring slope is not as steep as it had been for the 18-year record, whereas the

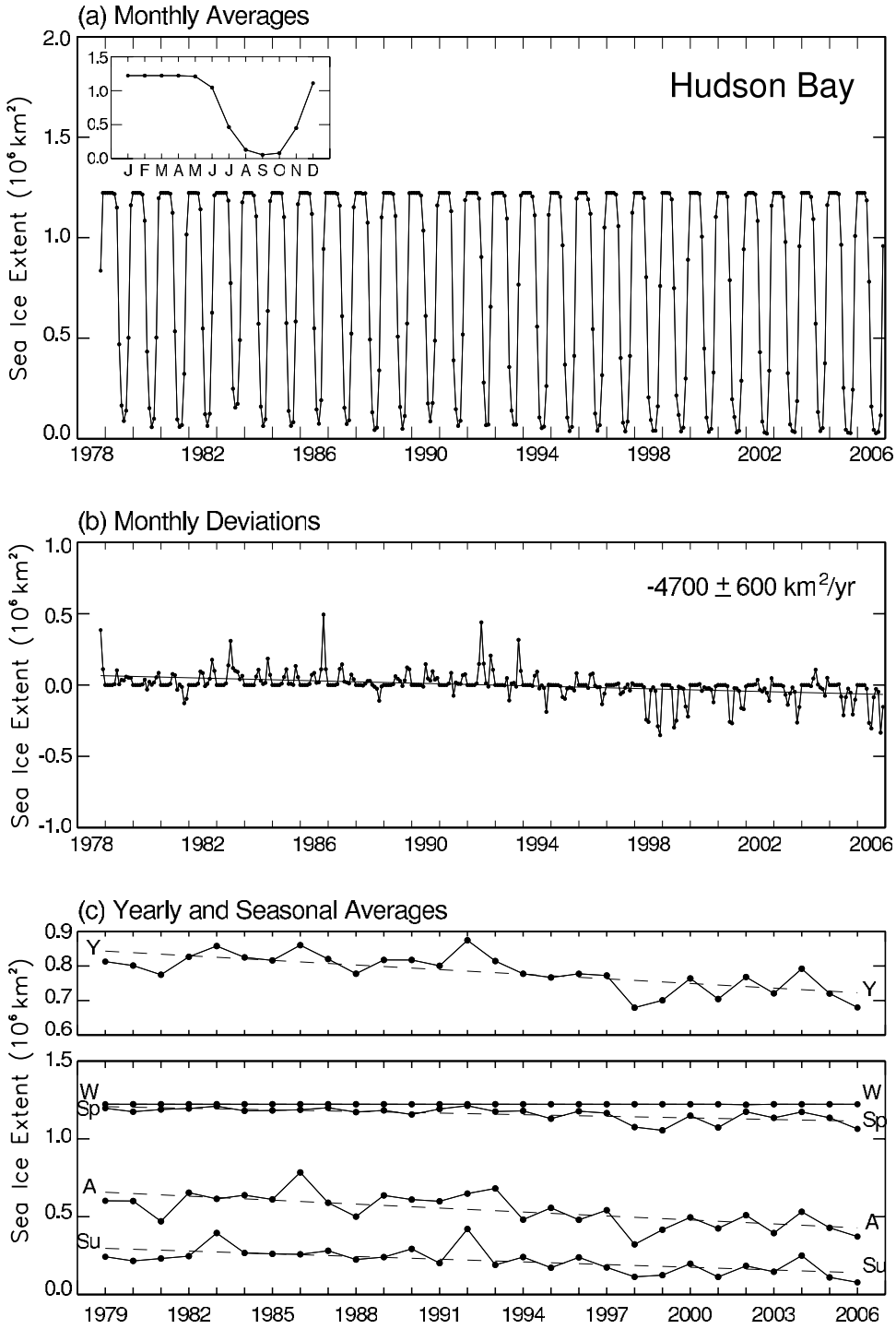

Figure 5. Same as Figure 2, except for the regional values for Hudson Bay.

slopes for the other three seasons and for the yearly average are all markedly steeper (Table 1 values versus those given by *Parkinson et al.* [1999]).

[10] On the basis of the individual months, the strongest 1979–2006 trend is for September, at $-56{,}800 \pm 9{,}700$ km^2/a, or -7.6 ± 1.3%/decade. This is slightly less steep than the value found by *Meier et al.* [2007] for 1979–2005, reflecting the slight rebounding of the September ice cover in 2006 versus 2005.

3.1.2. Regional Results

[11] Figures 3–11 present for each of the nine regions in turn, the corresponding results to those presented in Figure 2 for the Northern Hemisphere total; and Figure 12 presents, for each region and the total, plots showing the 28-year ice extent trends for each month. The ice extents in the seas of Okhotsk and Japan underwent marked overall decreases through 1997, although rebounded so rapidly in the next 4 years that the March value in 2001 was higher than any other monthly value throughout the 28-year record except

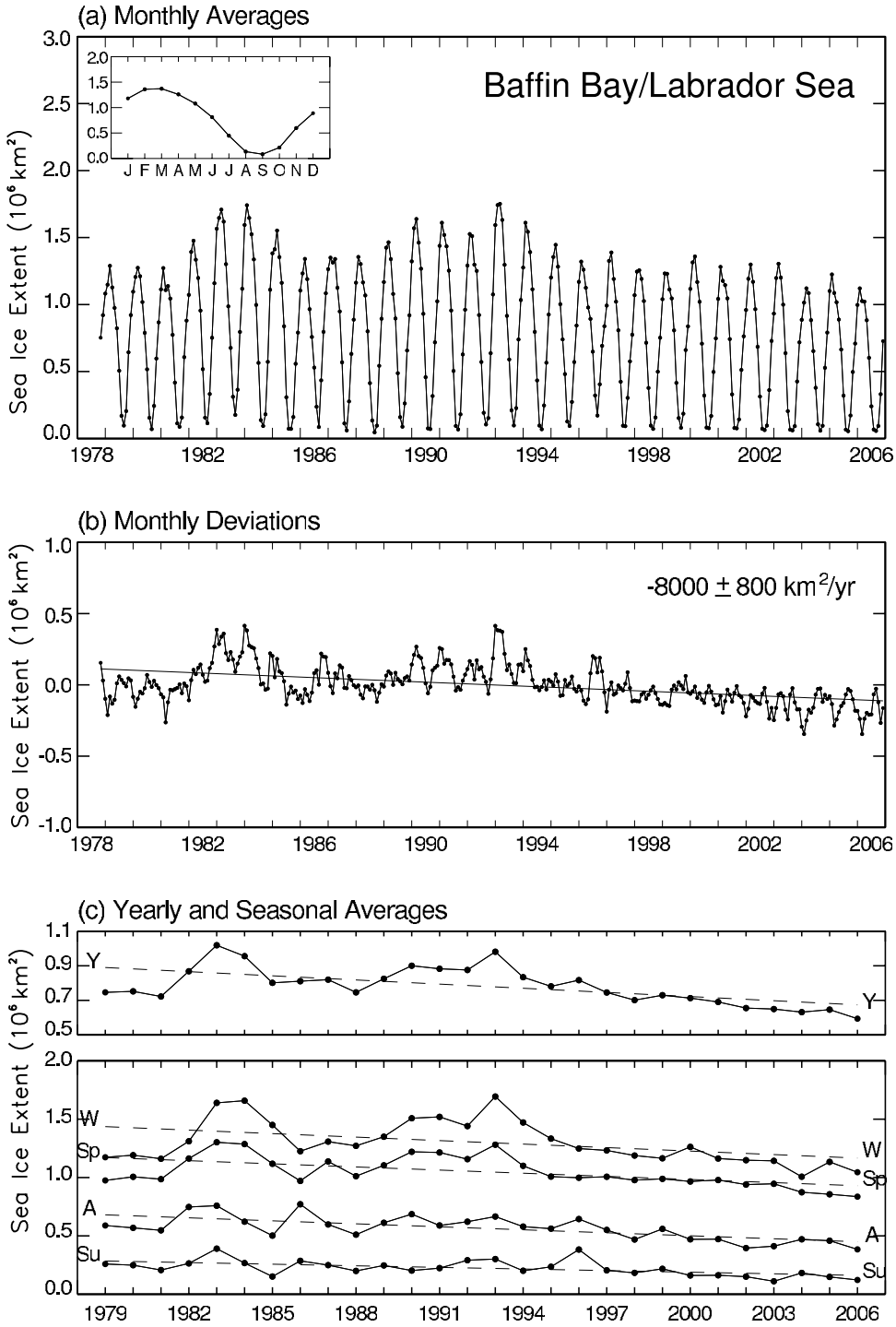

Figure 6. Same as Figure 2, except for the regional values for Baffin Bay/Labrador Sea.

for the February and March 1979 values (Figure 3a). This 2001 high point, however, was followed by monotonic winter-maximum decreases through the remainder of the record, i.e., through 2006 (Figure 3a). With the rebounding in 1997–2001, the negative slope of the monthly deviations, $-3{,}800 \pm 800$ km^2/a (Figure 3b), is far less steep than the $-9{,}700 \pm 1{,}400$ km^2/a slope reported for the record through 1996 [*Parkinson et al.*, 1999]. Still, the slopes remain negative, although at lesser significance levels (mostly 95% versus 99%) for the monthly deviations, yearly averages, and winter and spring seasons (Table 1), with the highest-magnitude slope occurring in April (Figure 12a). The slope is 0 in summer because of the absence of summer ice cover in each year.

[12] The Bering Sea results are dominated more by interannual variability than by long-term trends (Figure 4a), and consequently the trends are mostly not statistically significant (Table 1). The summer season, with the least amount of ice, has a statistically significant negative trend, but the negative trends in the monthly deviations, spring, autumn, and yearly average values and the positive trend in the winter values all fail the significance test (Figure 4b and

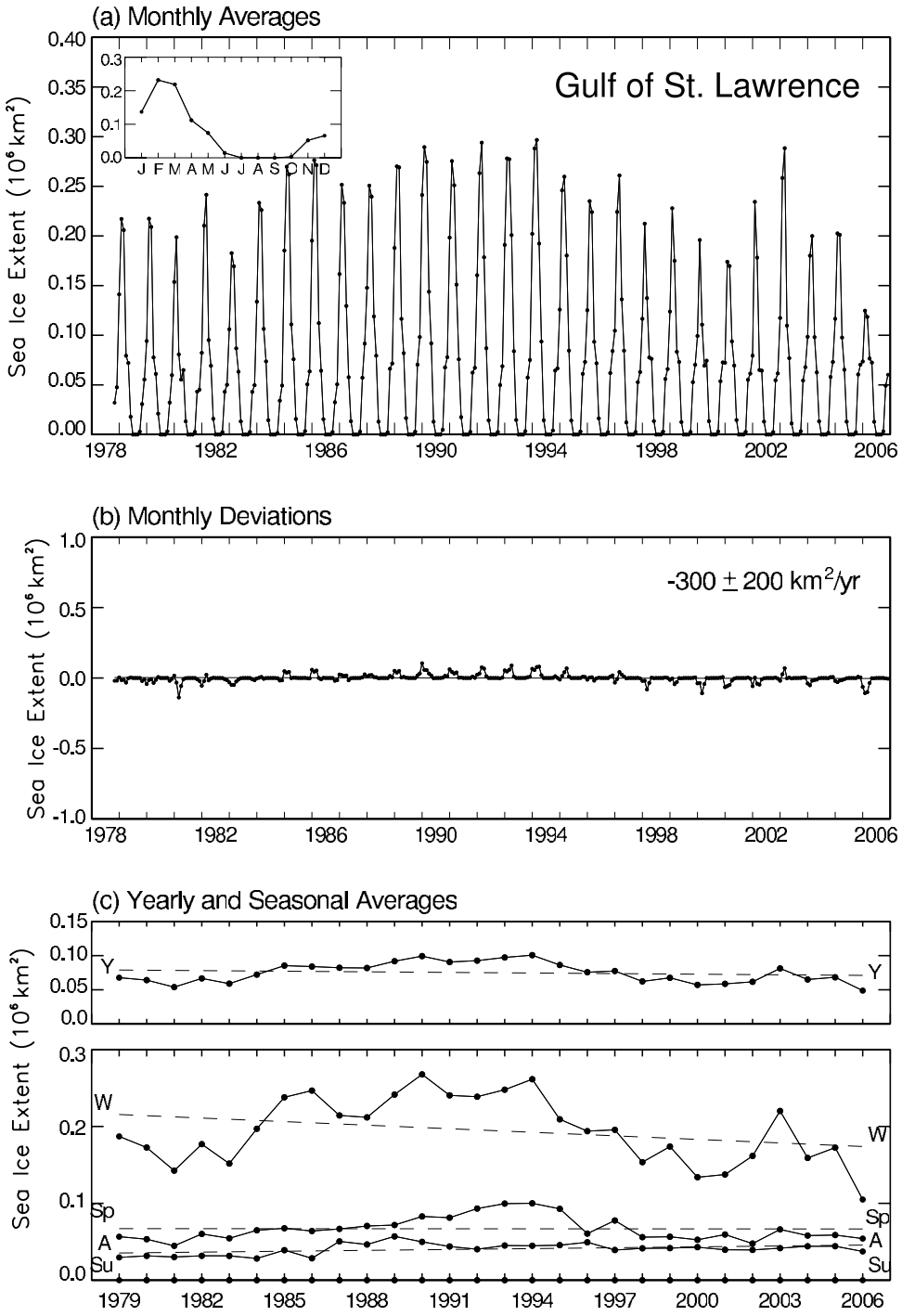

Figure 7. Same as Figure 2, except for the regional values for the Gulf of St. Lawrence.

Table 1). The strongest positive slope is in January, and the strongest negative slope is in March (Figure 12b). *Parkinson et al.* [1999] mention the occasional out-of-phase behaviors of the ice covers of the Bering Sea and seas of Okhotsk and Japan, relating them to atmospheric circulation and particularly the positioning of the Aleutian Low and Siberian High atmospheric pressure systems. Certainly a strong Aleutian Low positioned just to the east of the Kamchatka Peninsula would provide atmospheric forcing tending toward reduced ice coverage in the Bering Sea and expanded ice coverage in the Sea of Okhotsk, explaining why the two seas, although geographically separated only by the Kamchatka Peninsula, might have opposite changes. The recent years of the record continue to show occasional (but not persistent) out-of-phase behaviors, most notably in the yearly averages from 2003 through 2006, with monotonic decreases in the ice extents of the seas of Okhotsk and Japan and monotonic increases in the ice extents of the Bering Sea (Figures 3c and 4c). *Francis and Hunter* [2007] also highlight the importance of the Aleutian Low, although specifically for the wintertime Bering Sea ice cover for the 1979–2005 period.

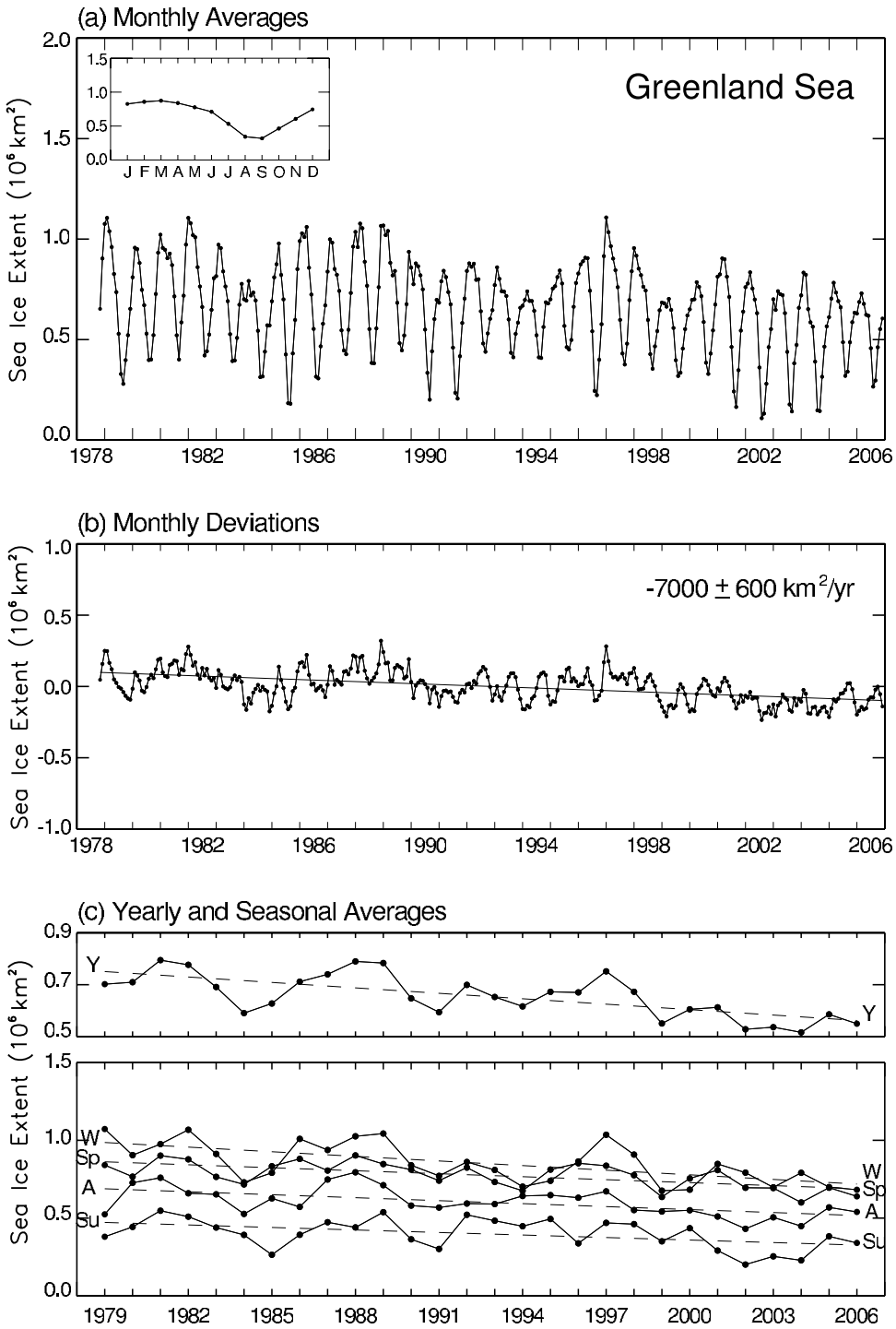

Figure 8. Same as Figure 2, except for the regional values for the Greenland Sea.

[13] Hudson Bay, overall, has been losing ice, with statistically significant negative trends in the monthly deviations, spring, summer, autumn, and yearly averages, and the lowest summer and second lowest spring, autumn, and annually averaged values of the 28-year record all coming in 2006, the final year of the record (Figures 5b and 5c and Table 1). The trend in the winter months is close to 0 (Figure 12c) because throughout the 28-year period, Hudson Bay has tended to be fully covered with ice in winter to at least 15% ice concentration. The decreasing ice coverage of Hudson Bay in the other months has been noted for its potentially detrimental impact on the Hudson Bay polar bear population [*Derocher et al.*, 2004; *Stirling and Parkinson*, 2006]. The very strong seasonal cycle, from full ice coverage in winter to near-zero ice coverage in late summer, and the large amount of winter ice coverage despite relatively low latitudes, are all tied to Hudson Bay's geographic location in the midst of the North American continent. Through the continentality effect, the region experiences colder winters

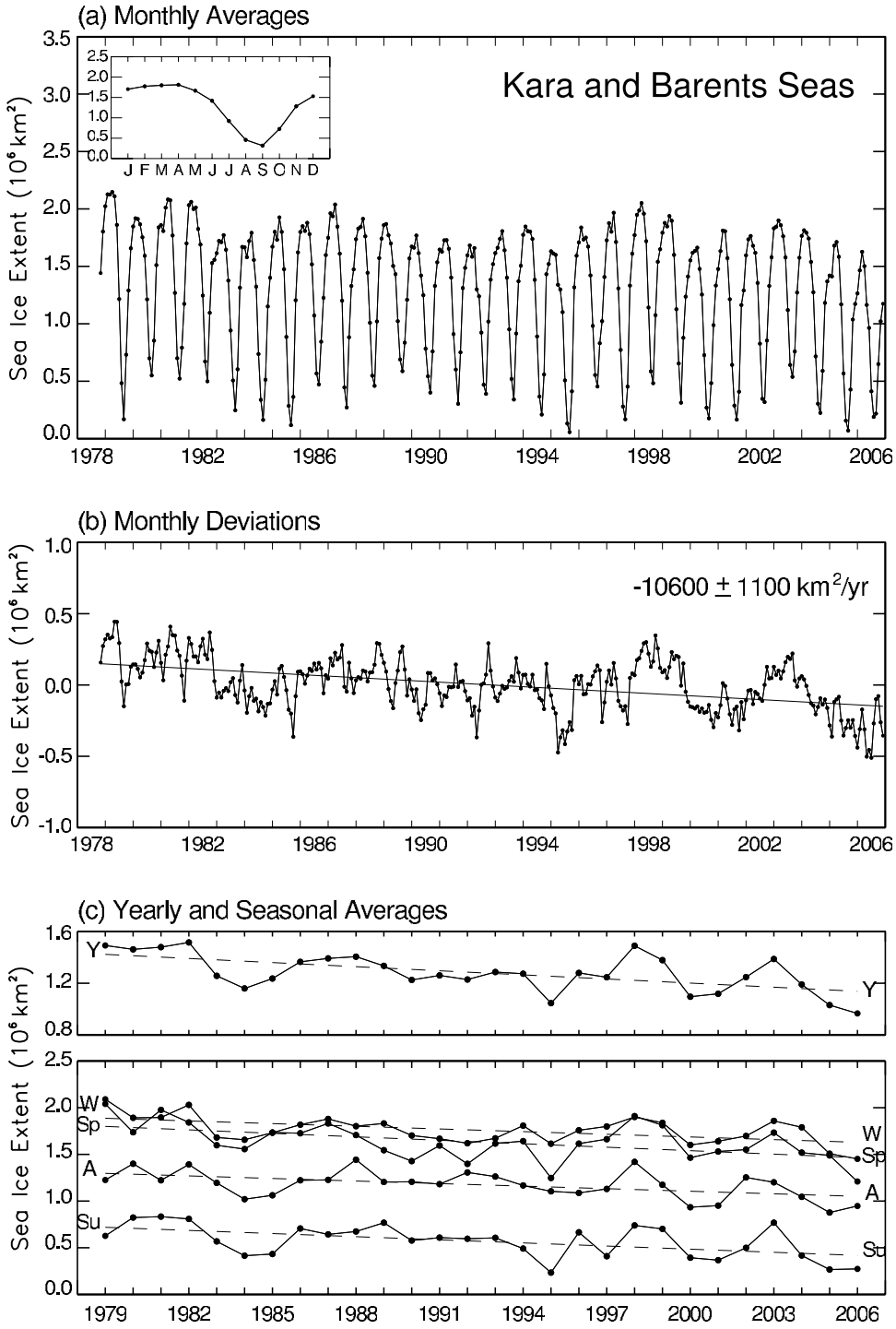

Figure 9. Same as Figure 2, except for the regional values for the Kara and Barents seas.

and warmer summers than midocean locations at comparable latitudes.

[14] The Baffin Bay/Labrador Sea region experienced a somewhat cyclical rise and fall of wintertime sea ice extents through two cycles of about 10 years each from 1979 through 1998, but a continuation of the cyclical pattern would have yielded a rise in ice extents over the next several years, which did not occur, being replaced instead, overall, by continued ice decreases (Figures 6a and 6c). The net result includes statistically significant negative trends in the monthly deviations, yearly averages, and all four seasonal averages, all significant at 99% except the winter averages, which are significant at 95% (Figure 6b and Table 1). When the record had extended only through 1996, with ice extents showing a cyclical behavior, the yearly, winter, spring, and summer trends had all been positive, at statistically insignificant levels, with the autumn trend negative but also statistically insignificant [*Parkinson et al.*, 1999]. With the record extended through 2006, each month shows a negative trend, although the trend for September is weak (Figure 12d). *Mysak et al.* [1996] relate the heavy ice conditions in 1983–1984 to the strong El

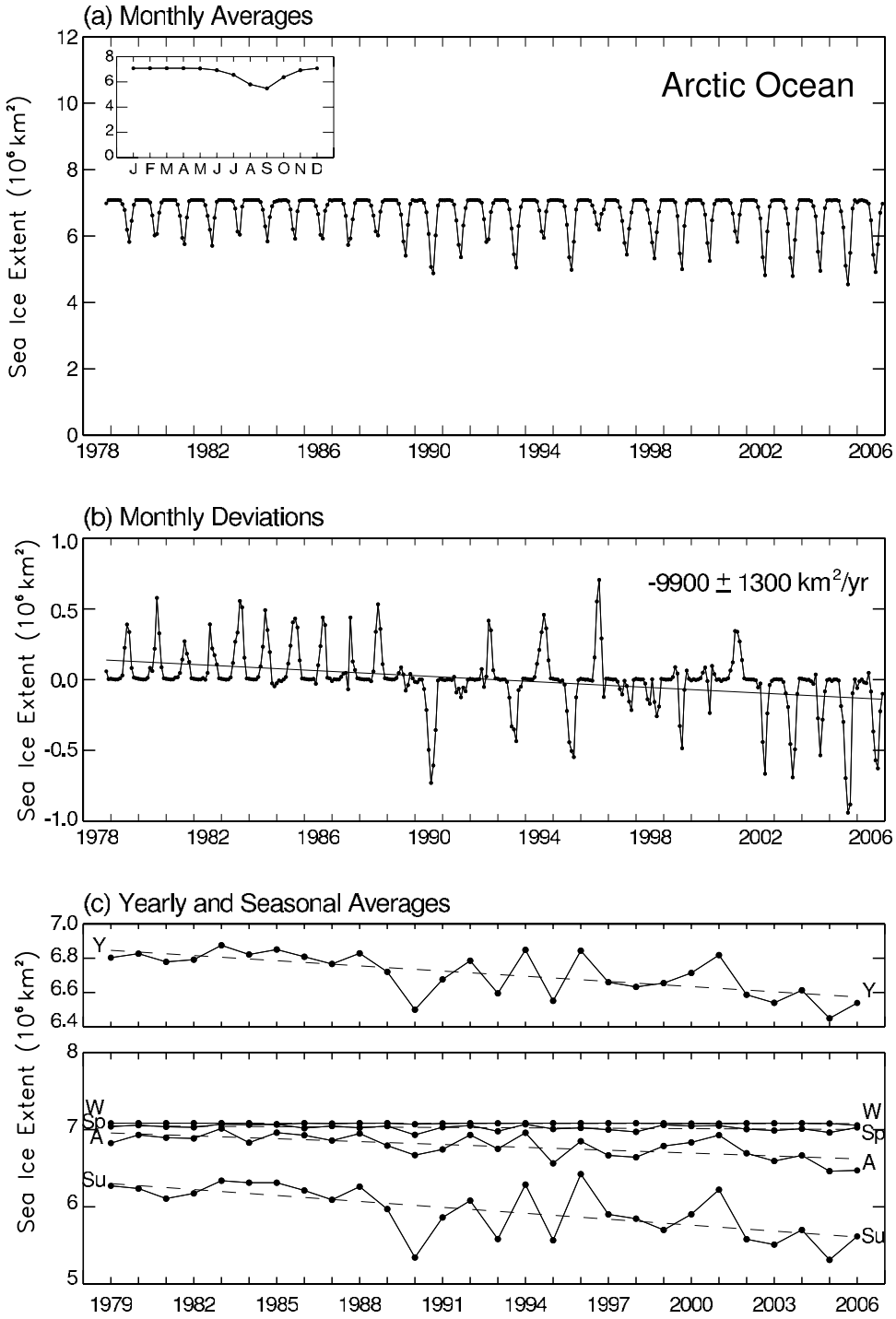

Figure 10. Same as Figure 2, except for the regional values for the Arctic Ocean.

Niño of 1982–1983, tied also to a deepened Icelandic Low and negative anomalies in the sea surface temperatures of Baffin Bay/Labrador Sea. They similarly relate the heavy ice coverage in the early 1990s to the lesser 1991–1992 El Niño and North Atlantic Oscillation (NAO; see section 5) event. The more recent ice record in Figure 6a, however, shows that the El Niño/sea ice correspondence broke down when the strong El Niño event of 1997–1998 was not soon followed by heavy ice coverage.

[15] The Gulf of St. Lawrence has by far the least ice coverage of any of the nine regions and has no ice in summertime. Its wintertime ice coverage was predominantly increasing through 1994, then decreased considerably through 2001, followed by marked increases the following 2 years, then much lower values in the final 3 years of the record (Figures 7a and 7c). The net result includes overall statistically insignificant negative trends in its monthly deviations, yearly average, winter, and spring values (Figure 7b and Table 1). In contrast, its autumn values show a positive trend with statistical significance at a 95% level. These replace what had been statistically significant positive trends through 1996 for the yearly, winter, spring,

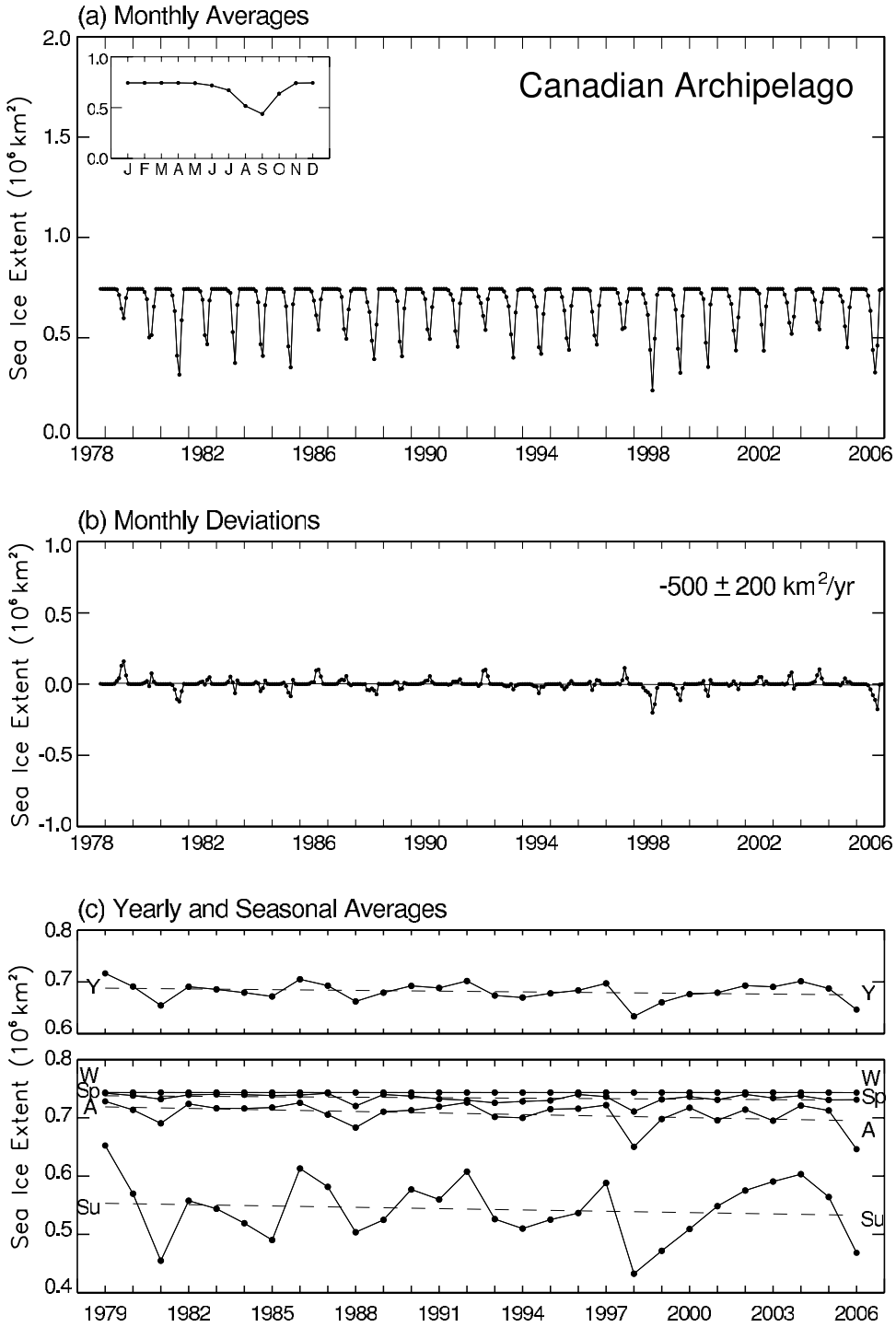

Figure 11. Same as Figure 2, except for the regional values for the Canadian Archipelago.

and autumn values [*Parkinson et al.*, 1999]. The positive autumn trends come from the ice increases in November and December, as the Gulf of St. Lawrence remains devoid of ice (or nearly so) in October, throughout the record, accounting for its 0 trend in October (Figure 12e).

[16] The Greenland Sea exhibits marked interannual variability in both its high and its low values, and even has several instances in which a high minimum is followed by a low maximum (e.g., summer 1993 and winter 1994) or vice versa (e.g., winter and summer 1994), both giving a small summer/winter contrast, and instances in which a low minimum is followed by a high maximum (e.g., summer 1996 and winter 1997) or vice versa (e.g., winter and summer 1979), giving a large summer/winter contrast. When these instances are sequenced in such a way that the summer/winter contrast increases, then decreases (or vice versa) over the course of several years, the plot exhibits a modulated wave pattern, as in the Greenland Sea case from 1993 to 1999 (Figure 8a). This behavior illustrates the incorrectness of assuming that particularly low ice coverage

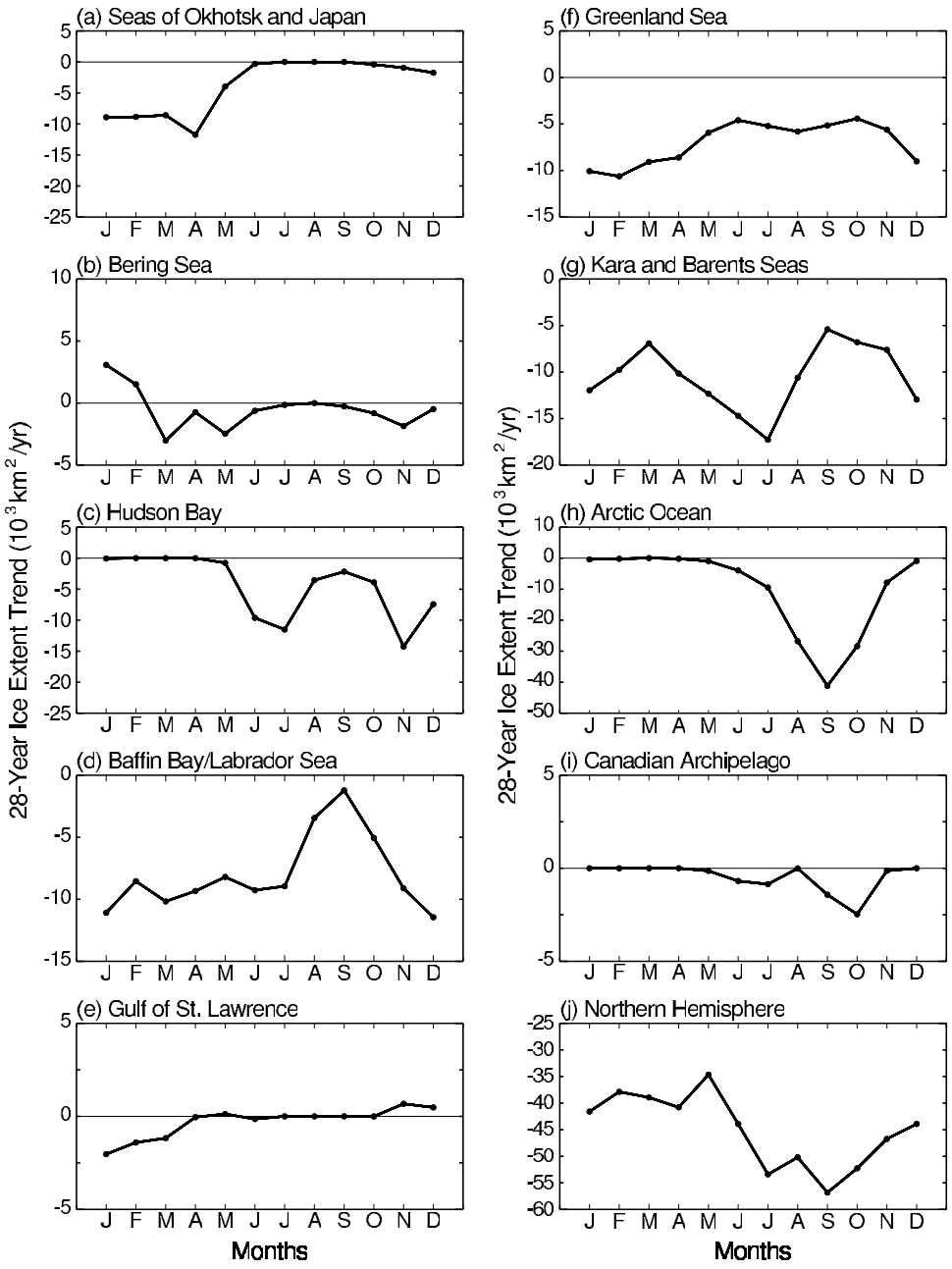

Figure 12. Sea ice extent trends by month over the 28-year period 1979–2006 for (a) seas of Okhotsk and Japan, (b) Bering Sea, (c) Hudson Bay, (d) Baffin Bay/Labrador Sea, (e) Gulf of St. Lawrence, (f) Greenland Sea, (g) Kara and Barents seas, (h) Arctic Ocean, (i) Canadian Archipelago, and (j) Northern Hemisphere total.

preconditions a region to continued low ice coverage. The Greenland Sea record clearly shows that low summertime ice is sometimes followed by low wintertime ice (e.g., summer 2002), sometimes by medium wintertime ice (e.g., summer 1991), and sometimes by high wintertime ice (e.g., summer 1996) (Figure 8a). Still, despite the variability, a negative trend is visible in the plots and is at a statistically significant level for the monthly deviations, the yearly averages, and each season (Figure 8 and Table 1). The trends are negative for every month, with the highest-magnitude trends in January and February (Figure 12f).

[17] The Kara and Barents seas also exhibit strong interannual variability and some short periods with the modulated wave behavior found also in the Greenland Sea in the ice extent record (Figure 9a). As with the Greenland Sea, despite the variability, negative trends are apparent throughout the year, in every month as well as every season (Figure 12g and Table 1). The negative trends are statistically significant at a 99% confidence level for the monthly deviations, yearly averages, and each season (Figure 9b and Table 1). The Kara and Barents seas region has the largest spring losses of any of the regions and is second only to the much larger Arctic Ocean in terms of summer ice loss. On a percentage basis, the summer ice cover of the Kara and Barents seas is losing 15.5 ± 5.0%/decade, which is considerably larger than the percentage loss in the Arctic Ocean

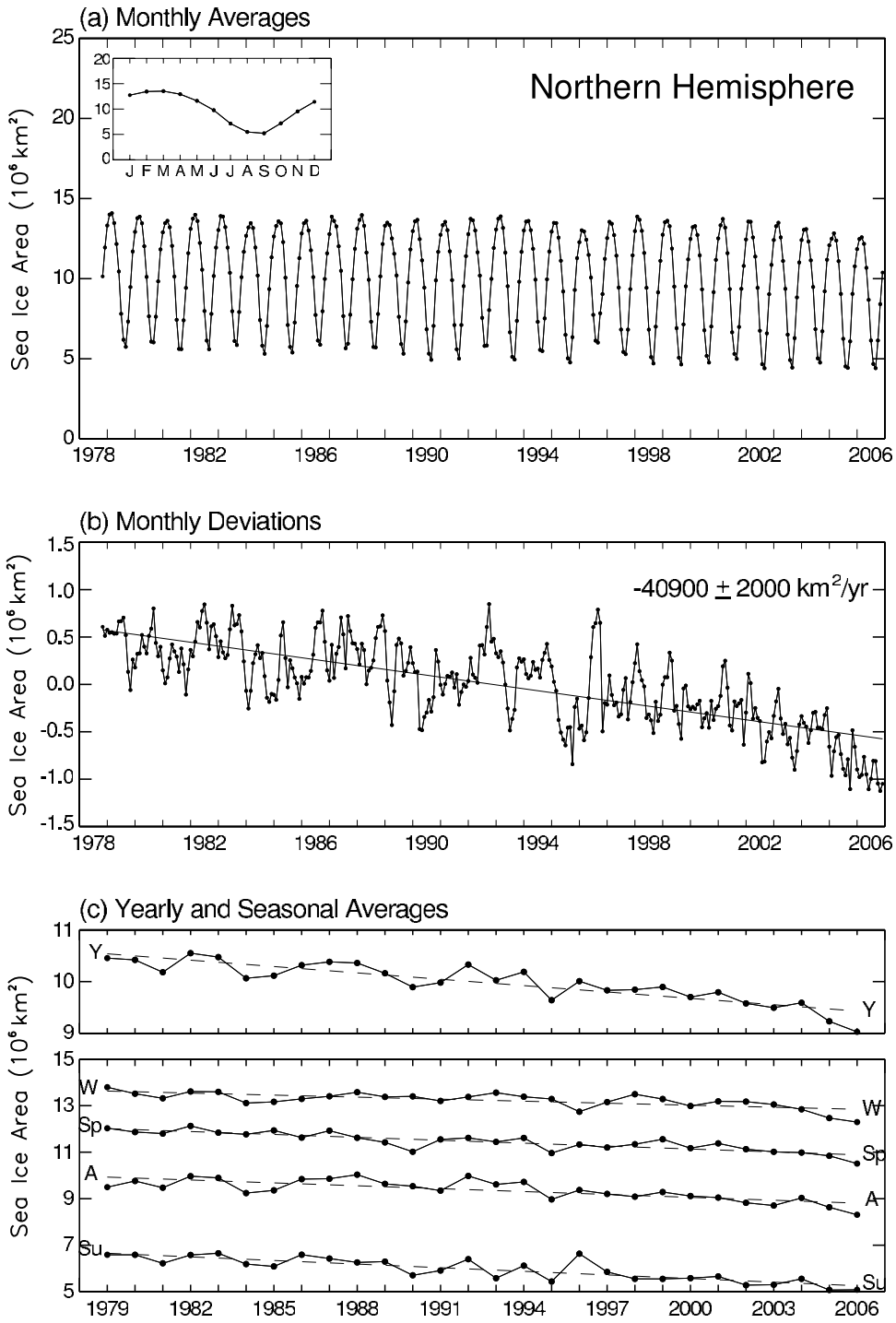

Figure 13. (a) Monthly averaged satellite-derived Northern Hemisphere sea ice areas for November 1978 through December 2006, with an inset presenting the average annual cycle. The average cycle reaches a minimum of 5.2 $\times$ 10^6 km^2 in September and a maximum of 13.5 $\times$ 10^6 km^2 in March. (b) Monthly deviations for the sea ice extents of Figure 13a, calculated as in Figure 2, plus the line of linear least squares fit through the monthly deviations, along with its slope and estimated standard deviation. (c) Yearly and seasonally averaged sea ice areas for the years 1979–2006. Seasons are defined as in Figure 2.

although is smaller than the percentage loss in the much lesser summertime ice covers of the Bering Sea, Hudson Bay, and Baffin Bay/Labrador Sea (Table 1). The wintertime ice losses in the Barents Sea have been connected to substantial wintertime sea surface temperature increases in this region [*Francis and Hunter*, 2007]. On a yearly average basis, the Kara and Barents seas ice losses, at $-10{,}600 \pm 2{,}800$ km^2/a, are larger even than those of the much larger Arctic Ocean (Table 1).

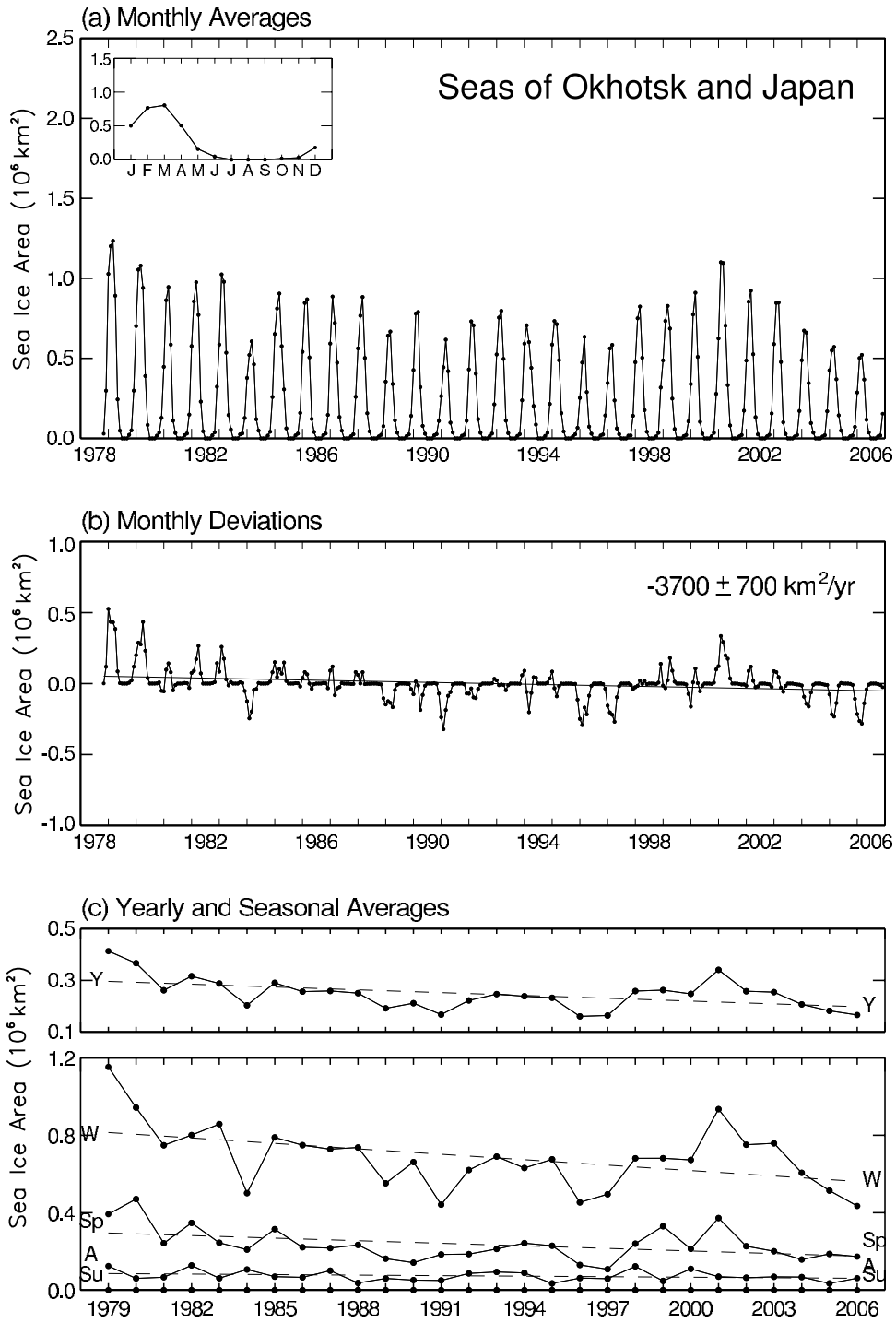

Figure 14. Same as Figure 13, except for the regional values for the seas of Okhotsk and Japan.

[18] The Arctic Ocean fills almost entirely with ice (to at least 15% ice concentration in almost all of the 25 × 25 km pixels) in the winter and much of the spring, and so the Arctic Ocean region's ice extent is capped each year at the value of the region's area, i.e., 7.08×10^6 km^2 (Figure 10a). As a result, the ice extent trends are at or very close to 0 for the winter results (Table 1) and for each of the months January–April (Figure 12h). There was a change to high variability in the summer and yearly average amounts between 1990 and 1996 (see *Maslanik et al.* [1996] and Figure 10c) and an overall increase of sea ice coverage during that time period and in fact through to 2001. Nonetheless, over the full 28-year record the Arctic Ocean ice cover experienced statistically significant decreases in its monthly deviations, yearly, summer, and autumn values at a 99% confidence level and in its spring values at a 95% confidence level (Figure 10b and Table 1). September is the month with by far the strongest negative trend (Figure 12h). *Maslanik et al.* [1996], *Comiso et al.* [2008], and *Stroeve et al.* [2008] all relate changes and variability in the Arctic

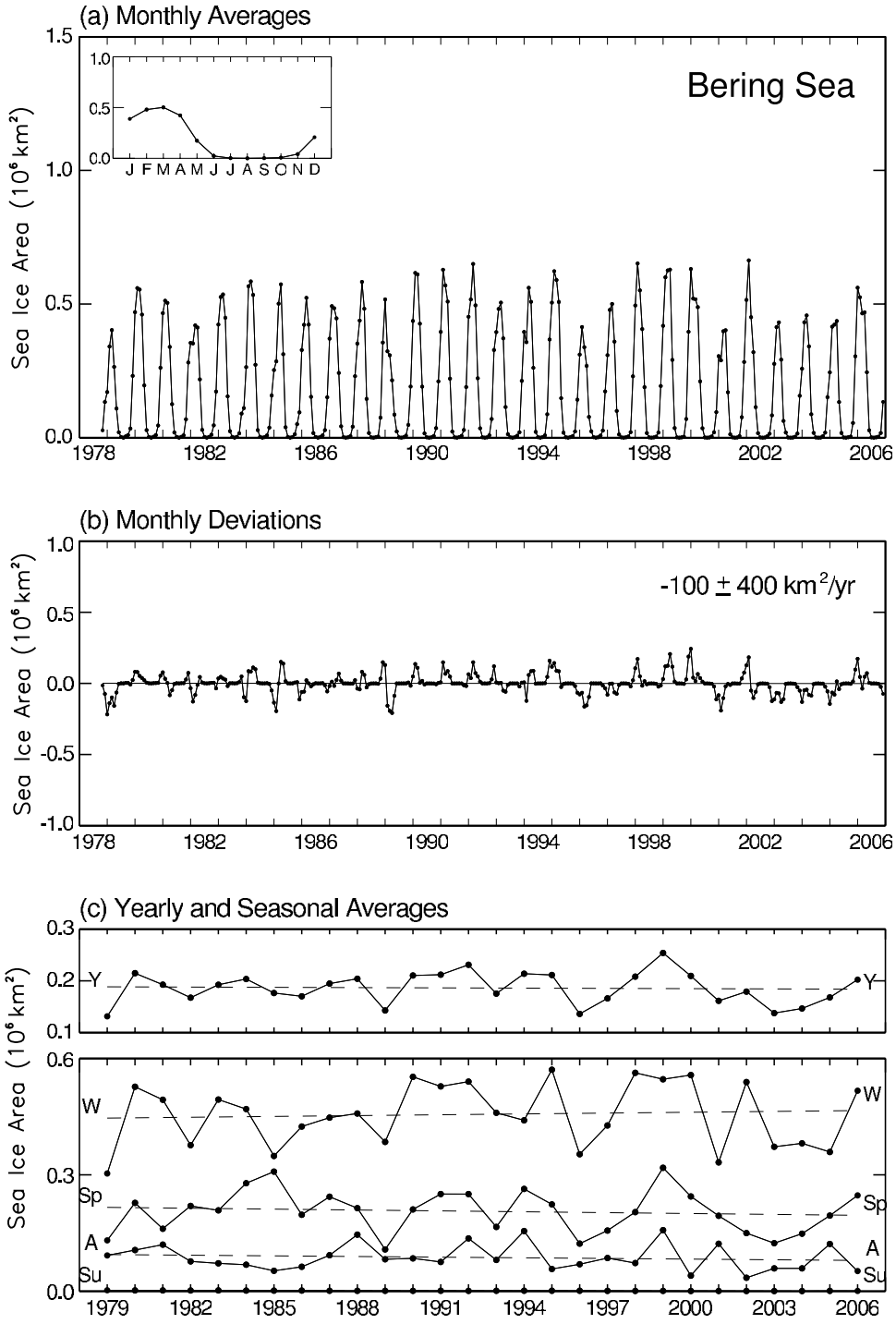

Figure 15. Same as Figure 13, except for the regional values for the Bering Sea.

Ocean summer ice cover to atmospheric forcing, as the winds have a significant effect both in moving the ice and in advecting warm air into the region.

[19] Finally, in the Canadian Archipelago the spring, summer, autumn, and yearly average ice extents all had their highest values in the first year of the record, 1979, but also had fluctuating rises and falls throughout the record (Figure 11c). The net result is negative trends without statistical significance for the yearly averages and each of the four seasons (Table 1). October has the strongest negative slope, followed by September (Figure 12i). The September decreases, at the annual minimum, have led in recent years to a dramatic potential impact on shipping, as the ice coverage in the Archipelago has reduced so much that a Northwest Passage has become quite feasible in many recent years.

3.2. Sea Ice Areas

[20] Sea ice area provides the total cumulative area of ice coverage, hence the total area over which the ice is directly insulating the ocean from the atmosphere and reflecting solar radiation. Corresponding to Figures 2–11 for the ice

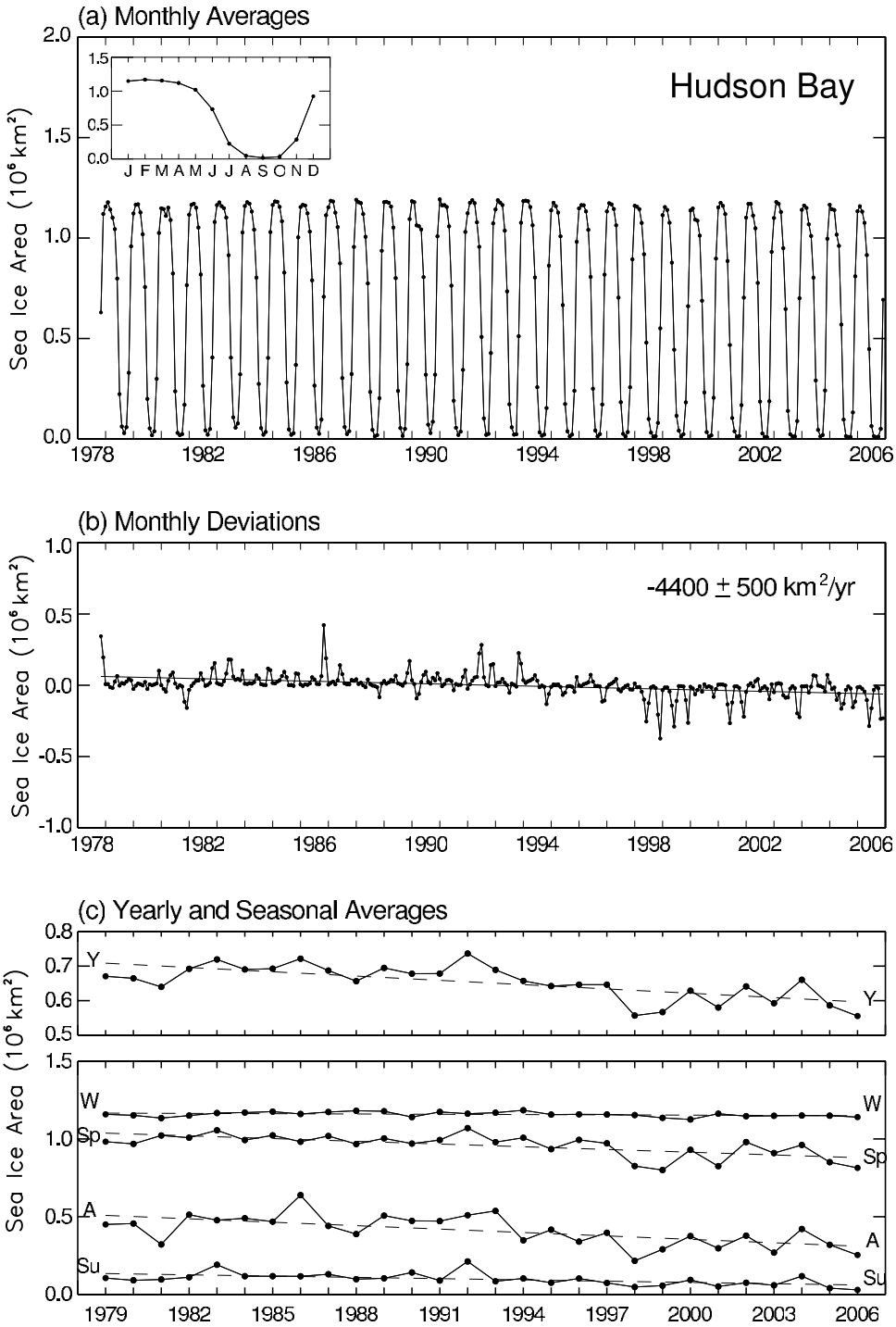

Figure 16. Same as Figure 13, except for the regional values for Hudson Bay.

extent, Figures 13–22 present the 28-year records of the ice area monthly averages, monthly deviations, and yearly and seasonal averages for the Northern Hemisphere total and for each of the nine regions. Similarly, corresponding to Table 1 and Figure 12 for ice extents, Table 2 presents the 28-year slopes of the lines of linear least squares fit through the yearly and seasonal ice area values for the Northern Hemisphere and each of the nine regions, and Figure 23 presents plots of the trend values for each month, again for the hemisphere and each region.

[21] Overall, the Northern Hemisphere ice areas track the ice extents very closely, although with all values shifted downward (Figure 13 versus Figure 2). (The only cases where ice area would not be less than ice extent would be cases in which throughout the entire region under consideration every pixel with at least 15% ice concentration had 100% ice concentration. This never occurs for the Northern Hemisphere as a whole and only occurs regionally in the essentially null case of a region having no ice, when the ice area and ice extent are equal at 0 km^2.) Like the ice extents,

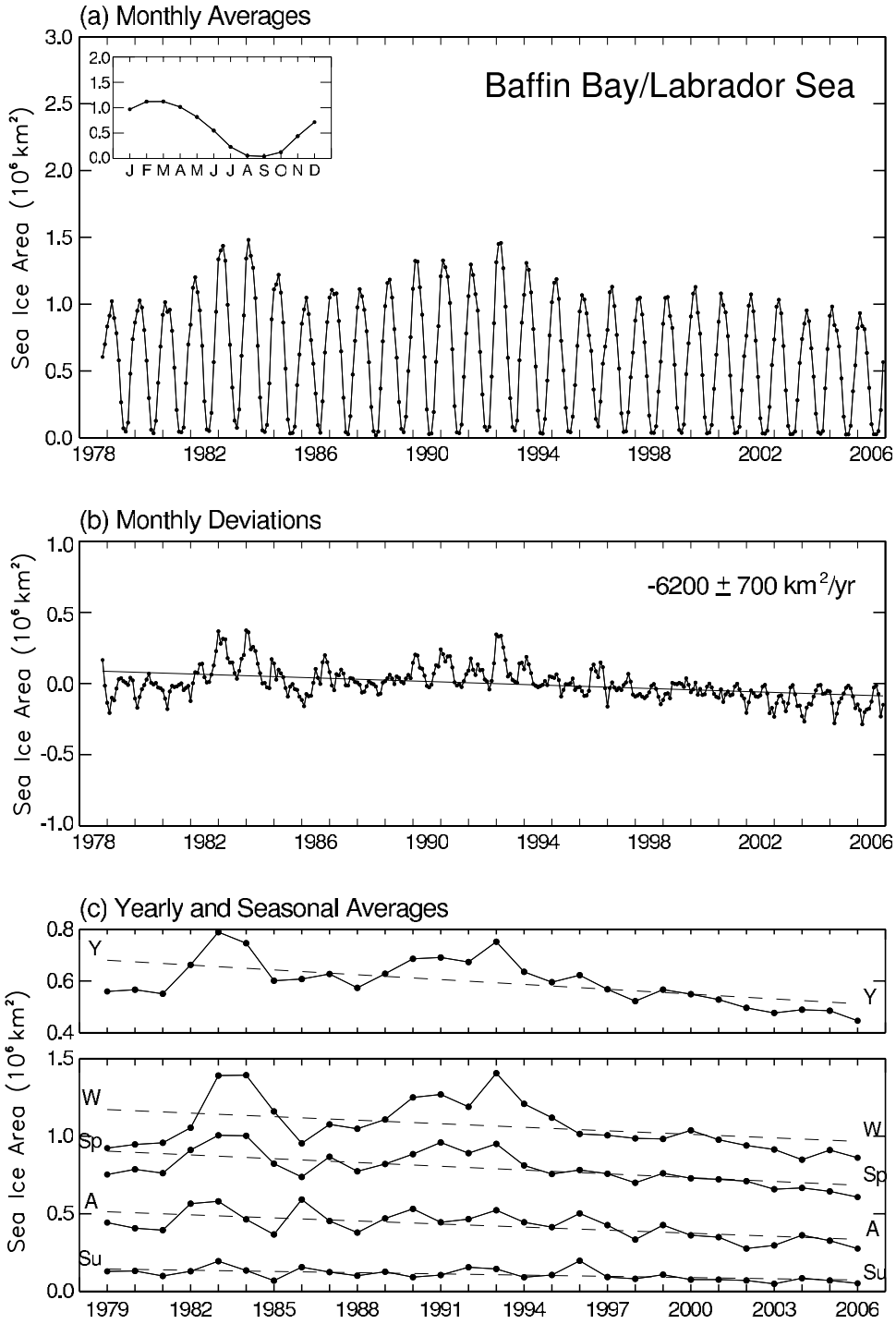

Figure 17. Same as Figure 13, except for the regional values for Baffin Bay/Labrador Sea.

the Northern Hemisphere sea ice areas exhibit statistically significant negative trends for the 28-year record for the monthly deviations, the yearly averages, and each of the four seasonal averages (Figure 13b and Table 2). The ice area negative slope is particularly steep for the summer season, at $-51{,}800 \pm 6{,}600$ km^2/a, although it is not as steep as the negative slope for the ice extents. This contrast is valid also for the winter and autumn seasons, with spring being the only season and May, June, and August the only months with a steeper slope in ice areas than in ice extents (Tables 1–2 and Figures 12j and 23j). This implies that in summer (as a whole, not August), autumn, and winter the ice concentrations, overall, have increased whereas in spring they have decreased. One mechanism that could potentially account for increasing ice concentrations with decreasing ice extents would be altered atmospheric circulation that increases the flow into the ice pack, hence promoting compaction.

[22] On a regional basis also, the ice area plots (Figures 14–22) track the ice extent plots (Figures 3–11)

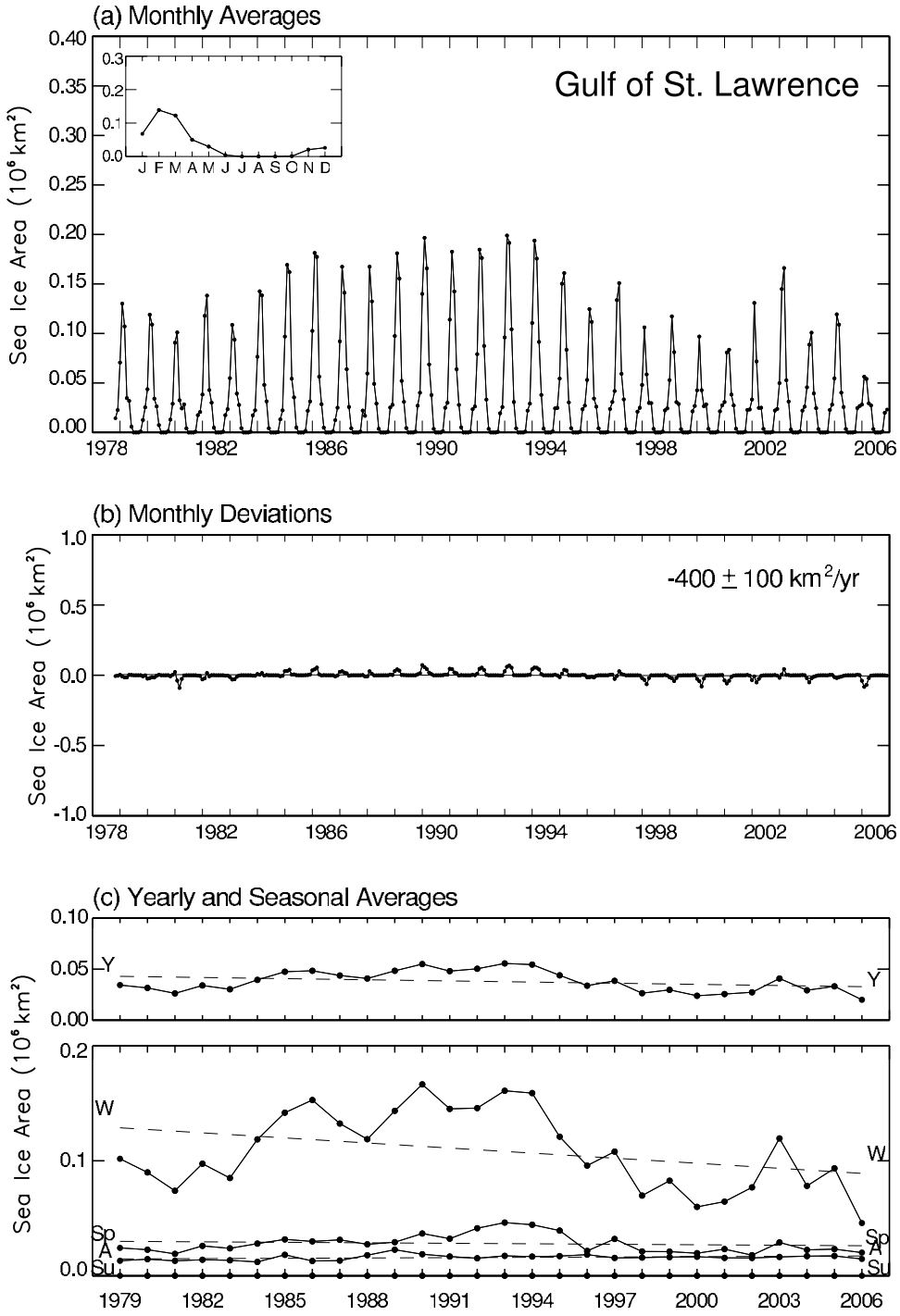

Figure 18. Same as Figure 13, except for the regional values for the Gulf of St. Lawrence.

quite closely, again with all values shifted downward. The tracking in the Greenland Sea, Arctic Ocean, and Canadian Archipelago is not as close as in the other regions, reflecting the high ice concentration variability in those regions. As with the ice extents, all ice area yearly trends are negative, with the Northern Hemisphere, Hudson Bay, Baffin Bay/Labrador Sea, Greenland Sea, Kara and Barents seas, and Arctic Ocean trends being statistically significant at a 99% level and the Gulf of St. Lawrence and Bering Sea trends not being statistically significant (Tables 1–2). The statistical significance for the seas of Okhotsk and Japan is at a 99% confidence level for the ice area results, versus 95% for the ice extent results, and the Canadian Archipelago ice area trend is statistically significant at a 95% confidence level, versus no statistical significance for the ice extent trend. The region with the largest ice area decrease, on a yearly average basis, is the Arctic Ocean, with a trend of $-11{,}600 \pm 2{,}400$ km^2/a, followed by the Kara and Barents seas, with a trend of $-9{,}600 \pm 2{,}600$ km^2/a, in reverse order from the largest ice extent losses. The fact that the negative trend for

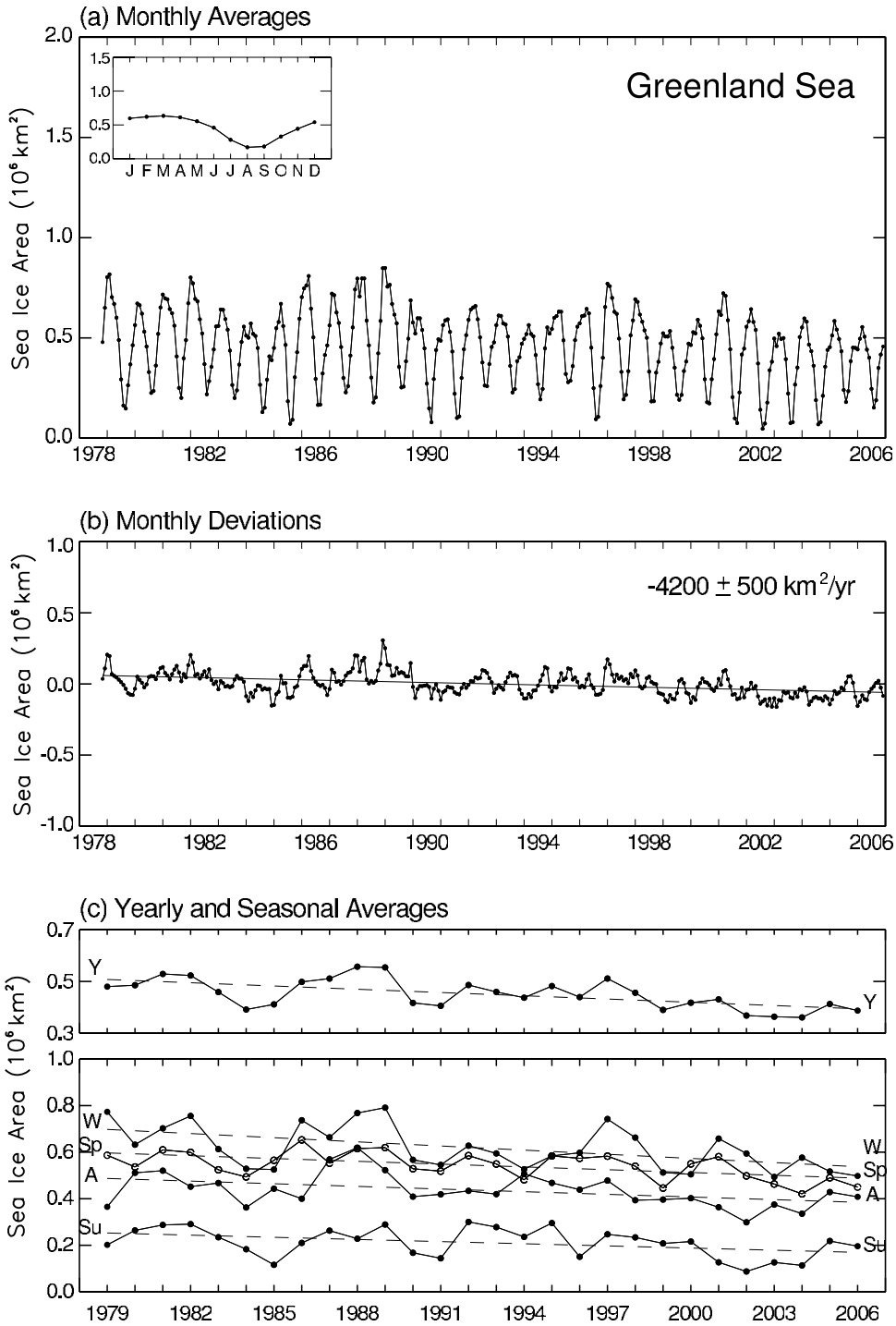

Figure 19. Same as Figure 13, except for the regional values for the Greenland Sea.

the Arctic Ocean has a larger magnitude for the ice areas than for the ice extents indicates that the ice concentrations, overall, have decreased in that region, whereas the fact that the negative trend for the Kara and Barents seas has a larger magnitude for the ice extents than the ice areas indicates that the ice concentrations, overall, have increased in that region. Although with lesser magnitudes involved, the Canadian Archipelago and Gulf of St. Lawrence conform with the Arctic Ocean in having reduced ice concentrations overall, whereas the remaining regions conform with the Kara and Barents seas in having increased ice concentrations overall. For the Northern Hemisphere as a whole, the greater ice extent decreases suggest increased ice concentrations for the reduced remaining ice cover (Tables 1–2).

[23] On a seasonal basis, the hemispheric increase in ice concentrations is valid for winter, summer, and autumn, although not for spring, for which season the concentrations instead decreased (Tables 1–2). On a seasonal basis also, the Arctic Ocean, Canadian Archipelago, and Northern Hemisphere as a whole had their greatest ice decreases in

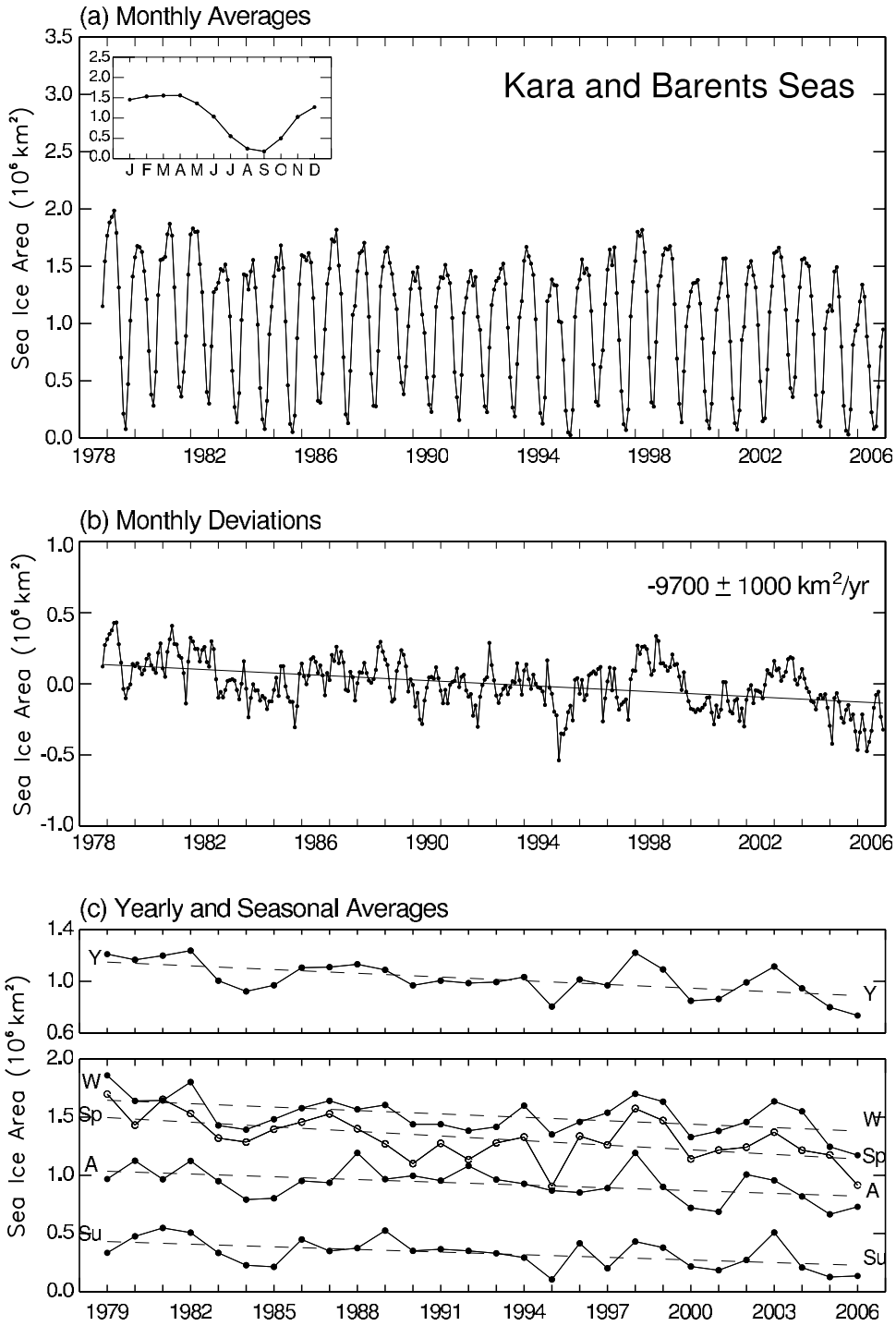

Figure 20. Same as Figure 13, except for the regional values for the Kara and Barents seas.

summer, but this was not true of the other seven regions. Specifically, the seas of Okhotsk and Japan, Greenland Sea, and the Gulf of St. Lawrence had their greatest decreases in winter; the Bering Sea, Baffin Bay/Labrador Sea, and Kara and Barents seas had their greatest decreases in spring; and Hudson Bay had its greatest decreases in autumn (Table 2; see Figure 23 for the month-by-month values and comparisons). On the basis of the magnitude of the ice area lost, in summer and autumn (when many of the regions have little ice to lose) the losses from the Arctic Ocean were largest, whereas in the winter and spring the losses from the Kara and Barents seas were largest, with the losses from the seas of Okhotsk and Japan a close second in the winter season (Table 2).

4. Summary

[24] The 28-year satellite passive-microwave record of Northern Hemisphere sea ice extents from 1979 through 2006 reveals decreases in the hemispheric ice extent in

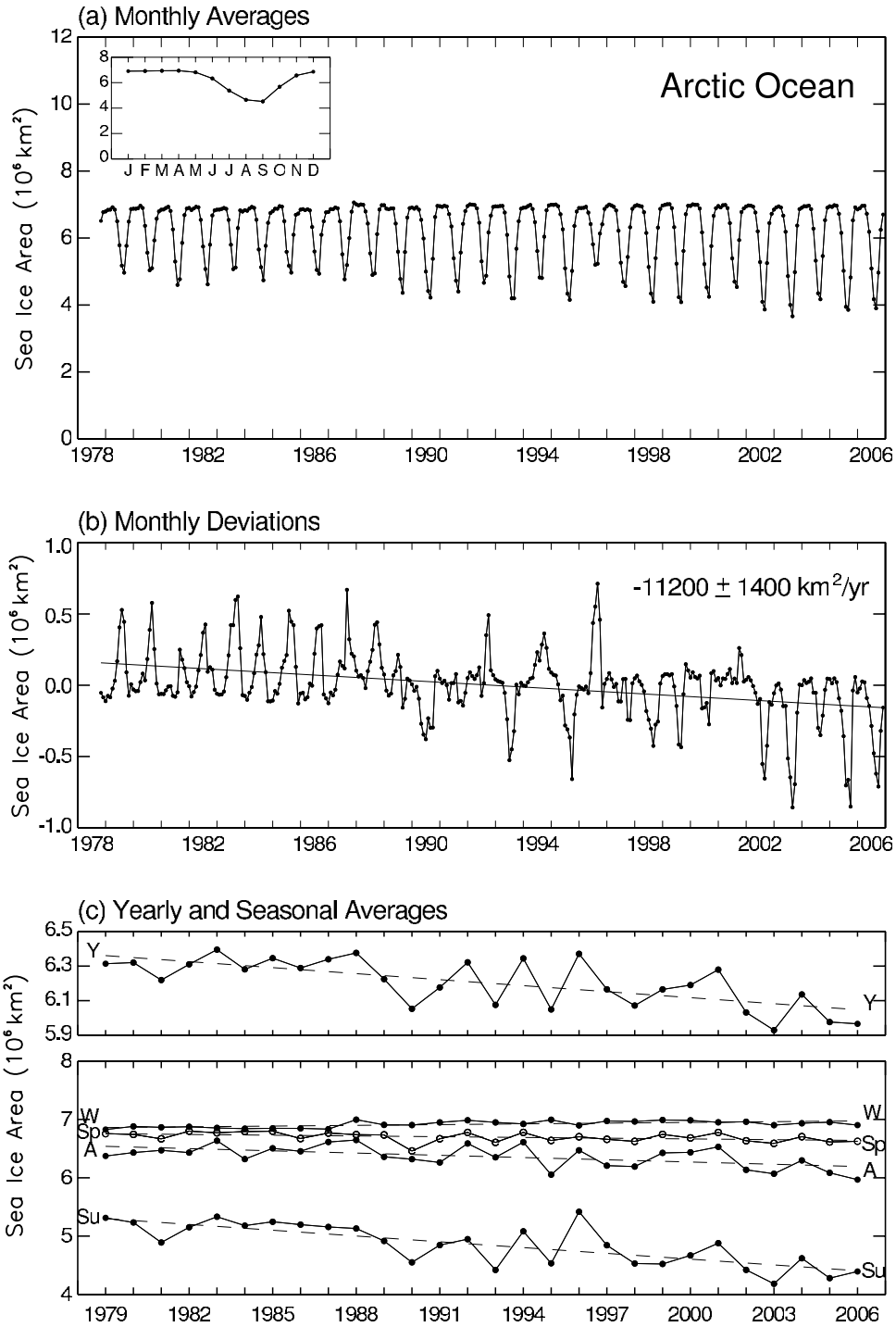

Figure 21. Same as Figure 13, except for the regional values for the Arctic Ocean.

every season and on a yearly average basis, with the slope of the least squares line through the yearly averages being $-45{,}100 \pm 4{,}600$ km^2/a (Table 1). The regions contributing the most to this yearly average decline are the Kara and Barents seas and the Arctic Ocean, although the largest percentage declines are in the Greenland Sea and Baffin Bay/Labrador Sea. On a seasonal basis, the largest contributors to the hemispheric ice decreases are Baffin Bay/Labrador Sea, the Greenland Sea, and the Kara and Barents seas in winter, the Kara and Barents seas in spring, the Arctic Ocean in summer, and the Arctic Ocean in autumn. All the regions have negative ice extent trends in the yearly averages, and the only seasonal positive trends are the autumn trend for the Gulf of St. Lawrence, and the winter trend for the Bering Sea (Table 1). On a month-by-month basis, the only positive trends are in January and February for the Bering Sea and in May, November, and December for the Gulf of St. Lawrence (Figure 12).

[25] The 28-year trends for ice areas are also all negative for the yearly averages but show statistically significant

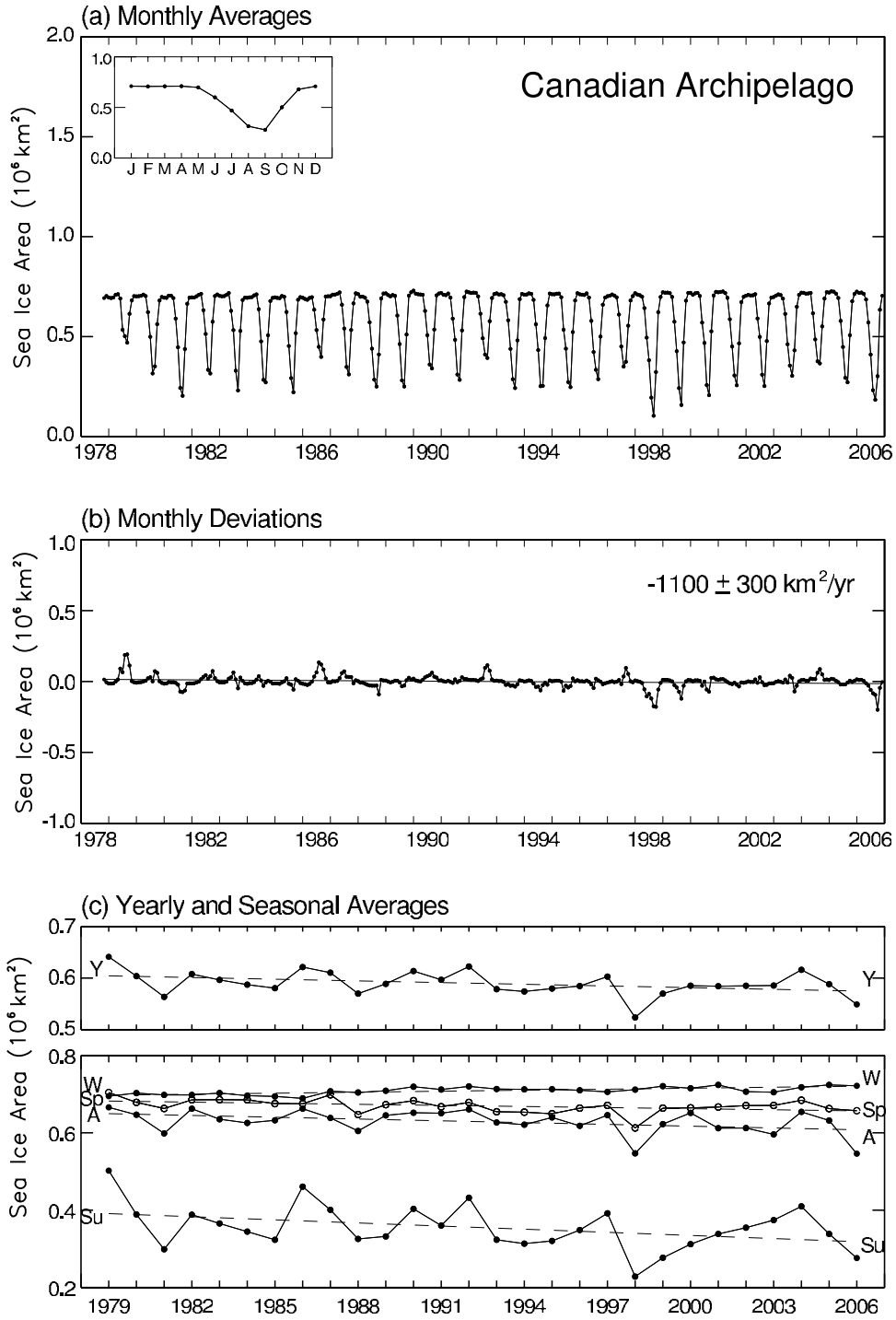

Figure 22. Same as Figure 13, except for the regional values for the Canadian Archipelago.

positive trends in winter for the Arctic Ocean and Canadian Archipelago and statistically insignificant positive trends in winter for the Bering Sea and in autumn for the Gulf of St. Lawrence (Table 2). The combined ice extent and ice area results indicate an increase in ice concentrations, overall hemispherically, in the winter, summer, and autumn seasons; that is, the much reduced sea ice cover has become somewhat more compact over the 1979–2006 period (Tables 1–2).

[26] Many of the numbers in this paper update numbers presented by *Parkinson et al.* [1999] for the 18-year record 1979–1996. The statistically significant slopes (at 95% confidence level or above) found for the 18-year ice extent record are decreasing trends in the yearly, winter, and spring averages of the Northern Hemisphere, the seas of Okhotsk and Japan, and the Kara and Barents seas, a decreasing trend in the winter averages of the Greenland Sea, decreasing trends in the summer averages of the Northern Hemisphere and the Bering Sea, and increasing trends in the

Table 2. Same as Table 1 Except for Sea Ice Areas Instead of Sea Ice Extents

Region	Yearly			Winter			Spring			Summer			Autumn		
	10^3 km^2/a	S	%/decade	10^3 km^2/a	S	%/decade	10^3 km^2/a	S	%/decade	10^3 km^2/a	S	%/decade	10^3 km^2/a	S	%/decade
Northern Hemisphere	−41.0 ± 4.3	99	−3.9 ± 0.4	−29.0 ± 5.7	99	−2.1 ± 0.4	−41.7 ± 4.9	99	−3.5 ± 0.4	−51.8 ± 6.6	99	−7.8 ± 1.0	−41.4 ± 6.8	99	−4.2 ± 0.7
Seas of Okhotsk and Japan	−3.6 ± 1.3	99	−12.3 ± 4.3	−9.4 ± 3.5	95	−11.5 ± 4.3	−4.4 ± 1.8	95	−15.0 ± 6.1	0.0 ± 0.0		0.0 ± 0.0	−0.9 ± 0.6		−10.5 ± 7.1
Bering Sea	−0.2 ± 0.7		−0.9 ± 3.9	0.7 ± 1.9		1.6 ± 4.3	−0.8 ± 1.3		−3.5 ± 6.1	−0.1 ± 0.0	99	−31.0 ± 3.0	−0.6 ± 0.8		−5.9 ± 8.5
Hudson Bay	−4.1 ± 0.9	99	−5.9 ± 1.2	−0.6 ± 0.3		−0.5 ± 0.3	−5.9 ± 1.3	99	−5.6 ± 1.3	−2.7 ± 0.8	99	−20.2 ± 6.0	−7.3 ± 1.9	99	−14.4 ± 3.6
Baffin Bay/Labrador Sea	−6.2 ± 1.7	99	−9.2 ± 2.5	−7.6 ± 3.5	95	−6.5 ± 3.0	−8.1 ± 2.0	99	−9.0 ± 2.2	−2.6 ± 0.8	99	−18.2 ± 5.2	−6.6 ± 1.6	99	−12.8 ± 3.2
Gulf of St. Lawrence	−0.4 ± 0.2		−8.7 ± 5.5	−1.5 ± 0.8		−11.4 ± 5.9	−0.1 ± 0.2		−4.7 ± 6.1	0.0 ± 0.0		0.0 ± 0.0	0.1 ± 0.1		6.5 ± 3.5
Greenland Sea	−4.2 ± 1.1	99	−8.3 ± 2.2	−5.9 ± 1.9	99	−8.5 ± 2.8	−4.0 ± 1.2	99	−6.7 ± 1.9	−3.1 ± 1.4	95	−12.2 ± 5.4	−3.8 ± 1.5	95	−7.8 ± 3.1
Kara and Barents Seas	−9.6 ± 2.6	99	−8.4 ± 2.2	−9.8 ± 3.2	99	−6.0 ± 2.0	−13.2 ± 3.7	99	−8.8 ± 2.5	−7.5 ± 2.6	99	−17.5 ± 6.1	−7.9 ± 2.9	95	−7.7 ± 2.8
Arctic Ocean	−11.6 ± 2.4	99	−1.8 ± 0.4	4.2 ± 1.0	99	0.6 ± 0.1	−4.2 ± 1.7	95	−0.6 ± 0.3	−33.1 ± 5.6	99	−6.2 ± 1.0	−12.8 ± 3.7	99	−2.0 ± 0.6
Canadian Archipelago	−1.1 ± 0.5	95	−1.8 ± 0.9	0.9 ± 0.2	99	1.2 ± 0.2	−0.9 ± 0.4	95	−1.4 ± 0.6	−2.7 ± 1.3	95	−6.9 ± 3.3	−1.5 ± 0.7	95	−2.4 ± 1.0

yearly, winter, spring, and autumn averages of the Gulf of St. Lawrence [*Parkinson et al.*, 1999, Table 1]. For each of the 18-year statistically significant negative trends, the trend remains negative and statistically significant in the 28-year record, but the Gulf of St. Lawrence retains a statistically significant positive trend only in the autumn results and has shifted to nonstatistically significant negative trends for the winter, spring, and yearly average values. With the longer record, additional negative slopes have become statistically significant (Table 1). Furthermore, for the hemisphere as a whole, the magnitude of the negative slope has increased, from the 1979–1996 to the 1979–2006 record, on a yearly average basis and in the winter, summer, and autumn, although not the spring. The nine regions show a mixed picture of slope increases and decreases between the original and extended record (Table 1 of *Parkinson et al.* [1999] versus Table 1).

5. Discussion: Sea Ice in a Larger Context

[27] Although tempered by interannual, regional, and seasonal variabilities, the 28-year Arctic sea ice record overall is one of prominent ice cover decreases (Tables 1–2 and Figures 2–23). Almost certainly these sea ice decreases have been caused in part by and have impacted the widespread Arctic warming [e.g., *Serreze et al.*, 2000; *Johannessen et al.*, 2004], as warmer temperatures increase melt and reduce freezing, and lessened ice cover allows more solar radiation to be absorbed in the Arctic climate system. In view of the interconnectedness of the ice/ocean/atmosphere system, it is also almost certain that the ice cover is impacted by large-scale oscillatory behaviors in the Arctic, including the North Atlantic Oscillation (NAO), defined as the oscillation in the difference of sea level pressure between the Icelandic Low and Azores High atmospheric pressure systems [*van Loon and Rogers*, 1978], and the Arctic Oscillation (AO), defined as the leading principal component of the wintertime monthly sea level pressure anomaly field north of 20°N [*Thompson and Wallace*, 1998]. The NAO is often regarded as the North Atlantic's regional representation of the AO.

[28] Numerous studies have attempted to connect the Northern Hemisphere sea ice variability with the NAO [e.g., *Deser et al.*, 2000; *Kwok*, 2000; *Parkinson*, 2000; *Partington et al.*, 2003] or the AO [e.g., *Deser et al.*, 2000; *Wang and Ikeda*, 2000; *Rigor et al.*, 2002; *Belchansky et al.*, 2004]. *Liu et al.* [2004] have further demonstrated a relationship between regional Arctic sea ice variability and both the AO and the El Niño/Southern Oscillation (ENSO), a global coupled ocean-atmosphere phenomenon first identified in the equatorial Pacific and South Pacific region. Specifically, *Liu et al.* show that the positive polarities of the AO and the occurrence of ENSO events result in similar changes in the western Arctic but opposite changes in the eastern Arctic. More importantly, the authors find that the magnitude of the sea ice variability associated with the AO and ENSO is much smaller than the observed regional ice trends. They suggest that in order to understand these regional trends it will be necessary to consider less understood large-scale processes and their nonlinear coupling to local-scale processes.

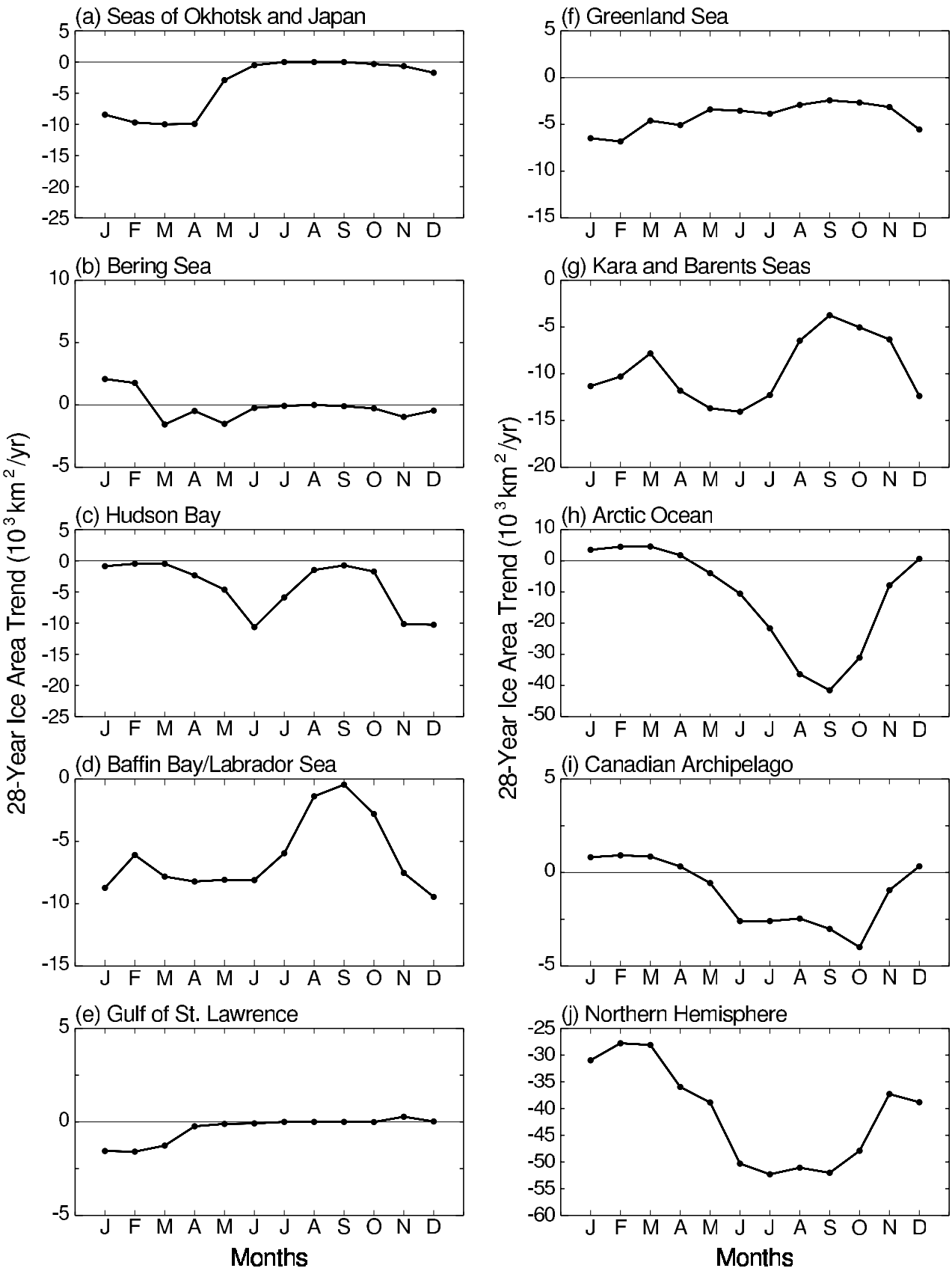

Figure 23. Sea ice area trends by month over the 28-year period 1979–2006 for (a) seas of Okhotsk and Japan, (b) Bering Sea, (c) Hudson Bay, (d) Baffin Bay/Labrador Sea, (e) Gulf of St. Lawrence, (f) Greenland Sea, (g) Kara and Barents seas, (h) Arctic Ocean, (i) Canadian Archipelago, and (j) Northern Hemisphere total.

[29] In a more recent study, *Ukita et al.* [2007] address the issue of regional Arctic sea ice variability and the larger-scale modes of atmospheric variability. They reveal a highly coherent spatial and temporal structure in Northern Hemisphere wintertime sea ice variability based on analysis of twenty-five winters of Arctic sea ice data. The dominant mode of this variability is characterized by a double-dipole composed of one dipole over the North Atlantic and the other dipole over the North Pacific, the two dipoles being mutually correlated on interannual timescales. The authors determine that this dominant sea ice mode is lag correlated with the winter-averaged NAO index at lags up to two winters when the NAO leads. Their analyses also reveal significant lead–lag relationships in sub-Arctic sea ice extent anomalies, which are argued to be indicative of an eastward propagating signal. One signal propagates from the Labrador Sea to the Nordic seas over one winter and another signal propagates from the Nordic seas to the Sea of Okhotsk over a second winter, thus linking regional sea ice variability across the Northern Hemisphere.

[30] The wintertime sea ice extents presented in the current paper provide uneven evidence of these dipole relationships, with the stronger correspondence coming early in the period covered. The Pacific dipole corresponds to the out-of-phase relationship observed between the sea ice extents in the Bering Sea region and the region of the seas of Okhotsk and Japan (Figures 3–4), whereas the Atlantic dipole, illustrated by the out-of-phase sea ice extent variations between the Baffin Bay/Labrador Sea region and the region of the Kara and Barents seas (Figures 6 and 9), appears to be evident to some extent early on but not in the last decade or so. This suggests that some other forcing may have superseded the influence of these atmospherically driven dipoles. Furthermore, there is no obvious evidence in the time series presented here of a propagating signal from the Labrador Sea to the Nordic seas as suggested by *Ukita et al.* [2007], but a more detailed numerical analysis of the sea ice anomalies may be needed to observe this signal.

[31] Despite regional differences, the overall hemispheric trend is becoming less rather than more suggestive that oscillatory patterns might dominate, with the downward trend instead becoming more pronounced in recent years (Figures 2 and 13). The rapid sea ice decrease beginning in the mid-1990s is quite likely closely related to the rapid warming that has been observed in surface air temperature, both by contributing to the atmospheric warming through allowing more heat transfer from the ocean to the atmosphere and by responding to the warming. In fact, a comparison of *Przybylak* [2007, Table 1] with Table 1 of this study reveals that the highest surface air temperature anomalies by season generally correspond to trends in sea ice extent that are significant at the 95% or 99% levels for approximately the same region and season.

[32] The year 2007 experienced a further decline in the sea ice cover, with a plummeting of the ice in the summer and a new record minimum ice coverage. The 2007 situation has been described by *Comiso et al.* [2008] and *Stroeve et al.* [2008], with both papers attributing the unusual decreases not just to warming but also to atmospheric circulation patterns conducive to ice retreat. *Comiso et al.* [2008] further show that the ice growth in the four weeks following the September record minimum had ice extents increasing at a rate that was at least as great as the rates for many of the earlier years in the satellite record; that is, the ice cover was recuperating somewhat from the anomalously large ice retreats.

[33] Projection into the future remains risky, but the loss of Arctic ice cover since the late 1970s is substantial, and if atmospheric temperatures continue to rise, as expected by the Intergovernmental Panel on Climate Change (IPCC) and others [*Meehl et al.*, 2007], then further loss of sea ice can be expected as well.

[34] In closing, we note that the Arctic ice decreases contrast markedly with the Antarctic results from the same data set. The Antarctic results are described in detail in a companion paper [*Cavalieri and Parkinson*, 2008] and show Southern Hemisphere sea ice extent and sea ice area increases. The Antarctic sea ice increases are considerably smaller than (on the order of 25% of) the Arctic sea ice decreases; and one major region of the Antarctic, the Bellingshausen/Amundsen seas region, has experienced ice decreases rather than increases [*Cavalieri and Parkinson*, 2008], placing it more in line with the Arctic changes than the overall changes in the rest of the Antarctic. The Bellingshausen/Amundsen seas region and the Antarctic Peninsula constituting its eastern boundary have, like the Arctic, experienced prominent warming over the course of the satellite record, whereas such warming has not been apparent throughout much of the rest of the Antarctic sea ice region [*Vaughan et al.*, 2003]. Hence in both hemispheres, as expected, on a large-scale basis warming has been associated with sea ice decreases.

[35] **Acknowledgments.** We thank Nick DiGirolamo and Al Ivanoff of Science Systems and Applications, Incorporated (SSAI) for considerable help in processing the data; and we additionally thank Nick DiGirolamo for considerable help in generating the figures. We also thank two anonymous reviewers for their review comments and the Editor Bruno Tremblay and anonymous Associate Editor for their time and assistance. This work was supported by NASA's Cryospheric Sciences Program and by NASA's Earth Observing System (EOS).

References

Aagaard, K., and E. C. Carmack (1989), The role of sea ice and other fresh water in the Arctic circulation, *J. Geophys. Res.*, *94*(C10), 14,485–14,498, doi:10.1029/JC094iC10p14485.

Barry, R. G., M. C. Serreze, J. A. Maslanik, and R. H. Preller (1993), The Arctic sea ice-climate system: Observations and modeling, *Rev. Geophys.*, *31*(4), 397–422, doi:10.1029/93RG01998.

Belchansky, G. I., D. C. Douglas, and N. G. Platonov (2004), Duration of the Arctic sea ice melt season: Regional and interannual variability, 1979–2001, *J. Clim.*, *17*, 67–80, doi:10.1175/1520-0442(2004)017<0067:DOTASI>2.0.CO;2.

Bjørgo, E., O. M. Johannessen, and M. W. Miles (1997), Analysis of merged SMMR-SSMI time series of Arctic and Antarctic sea ice parameters 1978–1995, *Geophys. Res. Lett.*, *24*(4), 413–416, doi:10.1029/96GL04021.

Cavalieri, D. J., and C. L. Parkinson (2008), Antarctic sea ice variability and trends, 1979–2006, *J. Geophys. Res.*, doi:10.1029/2007JC004564, in press.

Cavalieri, D. J., P. Gloersen, C. L. Parkinson, J. C. Comiso, and H. J. Zwally (1997), Observed hemispheric asymmetry in global sea ice changes, *Science*, *278*, 1104–1106, doi:10.1126/science.278.5340.1104.

Cavalieri, D. J., C. L. Parkinson, P. Gloersen, J. C. Comiso, and H. J. Zwally (1999), Deriving long-term time series of sea ice cover from satellite passive-microwave multisensor data sets, *J. Geophys. Res.*, *104*(C7), 15,803–15,814, doi:10.1029/1999JC900081.

Comiso, J. C. (2006), Abrupt decline in the Arctic winter sea ice cover, *Geophys. Res. Lett.*, *33*, L18504, doi:10.1029/2006GL027341.

Comiso, J. C., C. L. Parkinson, R. Gersten, and L. Stock (2008), Accelerated decline in the Arctic sea ice cover, *Geophys. Res. Lett.*, *35*, L01703, doi:10.1029/2007GL031972.

Derocher, A. E., N. J. Lunn, and I. Stirling (2004), Polar bears in a warming climate, *Integrative Comparative Biol.*, *44*, 163–176, doi:10.1093/icb/44.2.163.

Deser, C., J. E. Walsh, and M. S. Timlin (2000), Arctic sea ice variability in the context of recent atmospheric circulation trends, *J. Clim.*, *13*, 617–633, doi:10.1175/1520-0442(2000)013<0617:ASIVIT>2.0.CO;2.

Francis, J. A., and E. Hunter (2007), Drivers of declining sea ice in the Arctic winter: A tale of two seas, *Geophys. Res. Lett.*, *34*, L17503, doi:10.1029/2007GL030995.

Geffen, E., et al. (2007), Sea ice occurrence predicts genetic isolation in the Arctic fox, *Mol. Ecol.*, *16*(20), 4241–4255, doi:10.1111/j.1365-294X.2007.03507.x.

Gloersen, P., and W. J. Campbell (1991), Recent variations in Arctic and Antarctic sea-ice covers, *Nature*, *352*, 33–36, doi:10.1038/352033a0.

Johannessen, O. M., M. Miles, and E. Bjørgo (1995), The Arctic's shrinking sea ice, *Nature*, *376*, 126–127, doi:10.1038/376126a0.

Johannessen, O. M., et al. (2004), Arctic climate change: Observed and modelled temperature and sea-ice variability, *Tellus, Ser. A*, *56*(4), 328–341.

Kwok, R. (2000), Recent changes in Arctic Ocean sea ice motion associated with the North Atlantic Oscillation, *Geophys. Res. Lett.*, *27*(6), 775–778, doi:10.1029/1999GL002382.

Liu, J., J. A. Curry, and Y. Hu (2004), Recent Arctic sea ice variability: Connections to the Arctic Oscillation and the ENSO, *Geophys. Res. Lett.*, *31*, L09211, doi:10.1029/2004GL019858.

Maslanik, J. A., M. C. Serreze, and R. G. Barry (1996), Recent decreases in Arctic summer ice cover and linkages to atmospheric circulation anomalies, *Geophys. Res. Lett.*, *23*(13), 1677–1680, doi:10.1029/96GL01426.

Meehl, G. A., et al. (2007), Global climate projections, in *Climate Change 2007: The Physical Science Basis. Contribution of Working Group I to the Fourth Assessment Report of the Intergovernmental Panel on Climate Change*, edited by S. Solomon et al., pp. 747–845, Cambridge Univ. Press, Cambridge, UK.

Meier, W. N., J. Stroeve, and F. Fetterer (2007), Whither Arctic sea ice? A clear signal of decline regionally, seasonally and extending beyond the satellite record, *Ann. Glaciol.*, *46*, 428–434, doi:10.3189/172756407782871170.

Mysak, L. A., R. G. Ingram, J. Wang, and A. van der Baaren (1996), The anomalous sea-ice extent in Hudson Bay, Baffin Bay and the Labrador Sea during three simultaneous NAO and ENSO episodes, *Atmos. Ocean*, *34*(2), 313–343.

NSIDC (1992), *DMSP SSM/I Brightness Temperatures and Sea Ice Concentration Grids for the Polar Regions on CD-ROM User's Guide*, *Spec. Rep. 1*, Natl. Snow and Ice Data Cent., Coop. Inst. for Res. in Environ. Sci., Univ. of Colorado, Boulder.

Parkinson, C. L. (1996), Sea ice, in *Encyclopedia of Climate and Weather*, vol. 2, edited by S. H. Schneider, pp. 669–675, Oxford Univ. Press, New York.

Parkinson, C. L. (2000), Recent trend reversals in Arctic sea ice extents: Possible connections to the North Atlantic Oscillation, *Polar Geogr.*, *24*(1), 1–12.

Parkinson, C. L., and D. J. Cavalieri (1989), Arctic sea ice 1973–1987: Seasonal, regional, and interannual variability, *J. Geophys. Res.*, *94*(C10), 14,499–14,523, doi:10.1029/JC094iC10p14499.

Parkinson, C. L., D. J. Cavalieri, P. Gloersen, H. J. Zwally, and J. C. Comiso (1999), Arctic sea ice extents, areas, and trends, 1978–1996, *J. Geophys. Res.*, *104*(C9), 20,837–20,856, doi:10.1029/1999JC900082.

Partington, K., T. Flynn, D. Lamb, C. Bertoia, and K. Dedrick (2003), Late twentieth century Northern Hemisphere sea-ice record from U.S. National Ice Center ice charts, *J. Geophys. Res.*, *108*(C11), 3343, doi:10.1029/2002JC001623.

Przybylak, R. (2007), Recent air-temperature changes in the Arctic, *Ann. Glaciol.*, *46*, 316–324, doi:10.3189/172756407782871666.

Rigor, I. G., J. M. Wallace, and R. L. Colony (2002), Response of sea ice to the Arctic Oscillation, *J. Clim.*, *15*, 2648–2663, doi:10.1175/1520-0442(2002)015<2648:ROSITT>2.0.CO;2.

Rind, D., R. Healy, C. Parkinson, and D. Martinson (1995), The role of sea ice in 2x CO_2 climate model sensitivity. Part I: The total influence of sea ice thickness and extent, *J. Clim.*, *8*(3), 449–463, doi:10.1175/1520-0442(1995)008<0449:TROSII>2.0.CO;2.

Santer, B. D., T. M. L. Wigley, J. S. Boyle, D. J. Gaffen, J. J. Hnilo, D. Nychka, D. E. Parker, and K. E. Taylor (2000), Statistical significance of trends and trend differences in layer-average atmospheric temperature time series, *J. Geophys. Res.*, *105*(D6), 7337–7356, doi:10.1029/1999JD901105.

Serreze, M. C., J. E. Walsh, F. S. Chapin III, T. Osterkamp, M. Dyurgerov, V. Romanovsky, W. C. Oechel, J. Morison, T. Zhang, and R. G. Barry (2000), Observational evidence of recent change in the northern high-latitude environment, *Clim. Change*, *46*, 159–207, doi:10.1023/A:1005504031923.

Stirling, I., and C. L. Parkinson (2006), Possible effects of climate warming on selected populations of polar bears (*Ursus maritimus*) in the Canadian Arctic, *Arctic*, *59*(3), 261–275.

Stroeve, J. C., M. C. Serreze, F. Fetterer, T. Arbetter, W. Meier, J. Maslanik, and K. Knowles (2005), Tracking the Arctic's shrinking ice cover: Another extreme September minimum in 2004, *Geophys. Res. Lett.*, *32*, L04501, doi:10.1029/2004GL021810.

Stroeve, J., M. Serreze, S. Drobot, S. Gearheard, M. Holland, J. Maslanik, W. Meier, and T. Scambos (2008), Arctic sea ice extent plummets in 2007, *Eos Trans. AGU*, *89*(2), 13–14, doi:10.1029/2008EO020001.

Taylor, J. R. (1997), Least-squares fitting, in *An Introduction to Error Analysis: The Study of Uncertainties in Physical Measurements*, 2nd ed., pp. 181–207, Univ. Sci. Books, Sausalito, Calif.

Thompson, D. W. J., and J. M. Wallace (1998), The Arctic Oscillation signature in the wintertime geopotential height and temperature fields, *Geophys. Res. Lett.*, *25*(9), 1297–1300, doi:10.1029/98GL00950.

Ukita, J., M. Honda, H. Nakamura, Y. Tachibana, D. J. Cavalieri, C. L. Parkinson, H. Koide, and K. Yamamoto (2007), Northern Hemisphere sea ice variability: Lag structure and its implications, *Tellus, Ser. A*, *59*, 261–272.

van Loon, H., and J. C. Rogers (1978), The seesaw in winter temperatures between Greenland and northern Europe. Part I: General description, *Mon. Weather Rev.*, *106*(3), 296–310, doi:10.1175/1520-0493(1978)106<0296:TSIWTB>2.0.CO;2.

Vaughan, D. G., G. J. Marshall, W. M. Connolley, C. Parkinson, R. Mulvaney, D. A. Hodgson, J. C. King, C. J. Pudsey, and J. Turner (2003), Recent rapid regional climate warming on the Antarctic Peninsula, *Clim. Change*, *60*, 243–274, doi:10.1023/A:1026021217991.

Wang, J., and M. Ikeda (2000), Arctic Oscillation and Arctic Sea-Ice Oscillation, *Geophys. Res. Lett.*, *27*(9), 1287–1290.

Zwally, H. J., J. C. Comiso, C. L. Parkinson, D. J. Cavalieri, and P. Gloersen (2002), Variability of Antarctic sea ice 1979–1998, *J. Geophys. Res.*, *107*(C5), 3041, doi:10.1029/2000JC000733.

D. J. Cavalieri and C. L. Parkinson, Cryospheric Sciences Branch/Code 614.1, NASA Goddard Space Flight Center, Greenbelt, MD 20771, USA. (claire.l.parkinson@nasa.gov)